SAUSAGE INSTABILITIES ON A FLOWING JET- AN EXPERIMENTAL STUDY

by

Douglas W. Lindstrom

B.Sc., University of British Columbia, 1969

A THESIS SUBMITTED IN PARTIAL FULFILMENT OF
THE REQUIREMENTS FOR THE DEGREE OF
MASTER OF SCIENCE
in the Department
of
PHYSICS

We accept this thesis as conforming to the
required standard

THE UNIVERSITY OF BRITISH COLUMBIA

April, 1971

In presenting this thesis in partial fulfilment of the requirements for an advanced degree at the University of British Columbia, I agree that the Library shall make it freely available for reference and study. I further agree that permission for extensive copying of this thesis for scholarly purposes may be granted by the Head of my Department or by his representatives. It is understood that copying or publication of this thesis for financial gain shall not be allowed without my written permission.

Department of Physics

The University of British Columbia
Vancouver 8, Canada

Date _____

"If anyone can explain it, ...
I'll give him sixpence. I
don't believe there's an atom
of meaning in it."

Lewis Carroll
"Alice's Adventures
in Wonderland"

Abstract

The microwave resonator technique has been successfully employed in the study of a liquid model of a z pinch. A liquid column has formed an integral part of a microwave cavity, and changes in the frequency of such a cavity have been used to study the growth rates of the current driven instability.

The growth rates of the instability are seen to be in agreement with the standard theory for the wavelength equal to three centimeters. It is also seen that a definite stabilization is reached for a finite pinch amplitude. A simple theory balancing compressive streamline forces and magnetic pressure show that the maximum pinched amplitude should grow as the square of the axial current, which is what was observed.

Table of Contents

List of Figures

List of Graphs and Plates

Acknowledgements

I would like to take this opportunity to sincerely thank my research supervisor, Dr. F. L. Curzon, for the invaluable supervision which he gave me throughout the course of this work. His many clever suggestions, and sometimes witty remarks pulled me through the especially depressing days when one is looking for a simple, but efficient solution to some experimental problems.

I would also like to thank the members of the Plasma Physics group for numerous, often entertaining discussions, on many topics, sometimes including my experiment. Among these, one George Ionides, provided many hours of help with my experimental work.

I would also like to thank Mr. D. Sieberg and Mr. R. Da Costa for their technical assistance in the course of this work. I would also like to thank Mr R. Haines for his patient instruction during my familiarization with the student workshop.

I would like to extend credit, and sincere thanks to Mr. D. Stevenson for the technical artwork

that he did for this thesis, notably Figures 4-6 to 4-8. I give the figure numbers so that his excellent work will not have to suffer because of my own, slightly inferior artwork.

I would also like to thank W.E.L, Trailer Mfg. of Summerland, British Columbia for the kind donation of fibreglass sinks and trays which proved invaluable in containing mercury spills, which I must add, sometimes occurred.

Finally, I would like to thank the National Research Council of Canada for their generous scholarship which kept me out of financial trouble while attending Graduate School at the University of British Columbia.

Chapter 1 Introduction

A large problem, perhaps the largest problem facing plasma physicists today is creating a long-lived, or stable, high temperature plasma. This is of paramount importance in fusion research. One method of attacking this problem which has received considerable attention is the 'z' pinch. This is the constriction of a plasma column by its self magnetic field generated when a large axial current passes through it. It has been experimentally found however that such an arrangement is unstable (12).* That is to say, small perturbations on the system grow, and the very narrow plasma column is destroyed.

The theoretical investigation of such a configuration is extremely difficult. However, a solution is realized if one assumes that the plasma is collision dominated (the M.H.D. approximation). For most unstable modes, the condition $\text{div } \underline{v} = 0$, where $\underline{v}$ is the velocity vector is satisfied, so that the plasma behaves as if it were incompressible.

Quantitative experimental investigations of the z pinch are also extremely difficult. The linearization conditions required by the existing theory are very difficult to meet, and the short time periods involved make experimental investigations nearly impossible.

* ( ) gives reference number cited on page 78.

Since for the most unstable modes the plasma is essentially incompressible, the question " why not use a conducting liquid to test the theory " naturally arises. The conducting liquid would have to be in the form of a column, and would also have to have a large axial current flowing through it to be a valid model. The linearization condition of essentially 'small waves' would not be difficult to attain.

Such is the basis of this thesis. A new technique whereby the conducting column becomes an integral part of a microwave cavity is shown to give satisfactory information as to the nature of the 'surface waves' on the liquid column. The column is a coaxial rod in a cylindrical cavity, and the change in shape of the column can be deduced from the changes in the resonant frequency of the cavity. The details of the calculation relating surface configurations of the column to resonant frequency changes are given in chapter 3 of this thesis.

Chapter 2 of this thesis gives the basic theory of the unstable liquid column. It is split into two parts- the first part gives the instability of the jet (as the column will hereafter be called) without any axial current so that the effects of surface tension can be seen; the second part gives the theory of the jet when a large

axial current flows through it. The effects of jet velocity are also discussed, where it is shown that a totally stable mode exists when the perturbation does not travel along with the jet; that is, the perturbation is stationary in the frame of reference of the laboratory.

As previously mentioned, chapter 3 gives the details on how the amplitude of surface waves on the jet can be related to changes in the resonant frequency of the cavity.

Chapter 4 is a detailed description of the equipment- its method of operation, its drawbacks, and some of the setbacks incurred before its final state was achieved.

Chapter 5 contains the results of the experimental investigation. The validity of the results is discussed.

Chapter 6 could be called the ' what's next ' chapter. Future goals for this experiment are proposed along with possible methods of attack.

Two appendices have been included in this thesis. One appendix outlines clearly the safety precautions that are mandatory when working with mercury. For instance, a clear recipe on "what to do in case of a spill" is included. The other appendix describes a small scale

nickel plating apparatus that was constructed. Nickel plating is one method of beating the corrosive properties of mercury, the liquid conductor used.

Chapter 2 The Unstable Jet

Methods of Approach to Stability Problems

There are basically two methods of looking at the stability to vibrations of fluid systems. (These vibrations may not necessarily be mechanical.) There is the method of perturbation analysis where all the variables in the governing equations for the system are allowed to vary by a small amount from their equilibrium values, and the ensuing behavior is then studied. This method is strictly a mathematical approach where one essentially looks at the stability of the solution of a set of equations with no insight into how the instability occurs. In this method, the perturbation is assumed to grow exponentially in time as

$$e^{\omega t}$$

and the system is said to be unstable when the real part of ω is positive.

The second method is an analysis based on the exchange of energy in the system. The change in potential energy in the system due to a deformation is analyzed, and if it increases, the kinetic energy and consequently the motion of the fluid decreases. This implies that the disturbance is damped out, or in other words, the system is stable. When the potential energy decreases as a result

of the perturbation, the kinetic energy and hence the motion increases, implying instability.

This does not yet give the growth rate of the disturbance. To find this, the kinetic energy must be calculated, and a Lagrangian for the system defined. Substituting this into Lagrange's equation of mechanics gives that the growth is exponential, and also gives the functional form of the growth rate.

The first method has received far more attention than the second. This presumably stems from the fact that the perturbation analysis is straightforward to apply, usually involving only simple differentiation, whereas the energy method is not as easy to apply, often containing complicated integrals which have to be evaluated.

Although the first method is easier to apply, it is my opinion that the second method is more legitimate. In the second method, the actual physics of the situation is kept constantly in mind, and instead of looking at the stability of a set of equations, one looks at the stability of the actual physical situation.

In what follows, the unstable jet is investigated for instabilities due to surface tension and large axial d.c. currents, using the above discussed energy method.

The Capillary Instability of a Liquid Jet

I shall now discuss the instability of a liquid column due strictly to capillary forces. The problem will be investigated from the exchange of energy approach.

Consider a very long cylinder of fluid in motion with uniform velocity $\underline{V_o}$. Suppose that the fluid is incompressible and inviscid, and further suppose that the only force tending to keep the jet in its cylindrical shape is due to the surface tension T of the fluid. That is, neglect gravity. Define the frame of reference and coordinate system moving with the fluid as shown in Fig. 2-1.

capillary jet

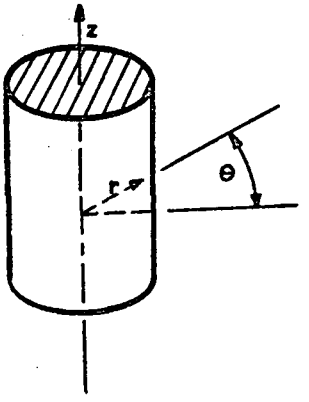

FIG. 2 - 1

Suppose that exterior to the jet is a vacuum, so that the pressure inside the jet, p_o, is given by

$$p_o = \frac{T}{R_o} \tag{1}$$

where R_o is the equilibrium radius of the column.

It is easy to see that the surface of such a configuration is unstable, for some disturbances at least. For consider an axi-symmetric 'squeezing' of the jet at some point. The jet will assume the form shown in Fig. 2-2.

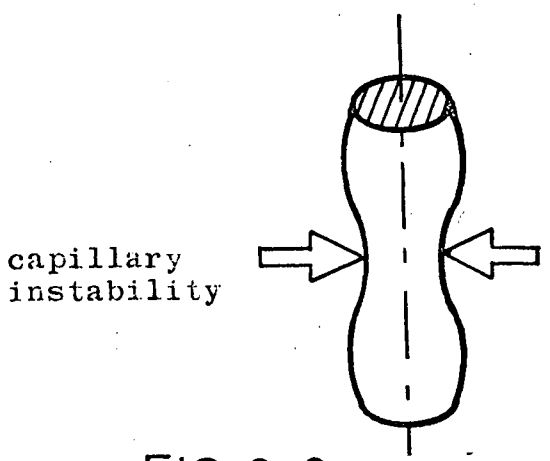

FIG. 2-2

In the region of the constriction, the radius of the jet is less. Consequently by equation (1), the pressure is greater in this region. This further constricts the jet, which further increases the pressure. Thus it is easy to see that the jet may well be unstable for certain disturbances on its surface.

I shall handle this simple problem by the energy method. First a disturbance will be placed on the surface of the jet. The change in potential energy of the system due to this surface deformation will then be calculated. When this is negative, the system is unstable.

Next, the kinetic energy will be calculated, and a Lagrangian for the system defined. The equations of motion will then be used to give the growth rate of the instability.

Consider the long column of fluid at rest in our chosen reference frame. The surface for the equilibrium state is given by

$$r = R_o$$

The disturbed surface can be represented by

$$r = R_1 + F(z,\Theta,t)$$

which owing to Fourier's theorem, can be written as

$$r = R_1 + \sum_m a_m(t)\, e^{i(k_m z + m\Theta)}$$

where k_m is identified with the wavenumber of the disturbance.

Because the governing equations are linear in their variables, we are justified in looking at just one mode, say $m = n$ and then summing if we want the general result. That is, consider a surface deformed to

$$r = R_1 + a_n(t)\, e^{i(k_n z + n\Theta)}$$

It is not clear that the average radius R_1 for the disturbed column is the same as the radius of the undisturbed column. In fact, $R_o \neq R_1$

to first order only in the perturbation amplitude, as can be seen from the following calculation.

Because the fluid is incompressible, the volume of a given element must always be constant;

ie. $$\pi R_o^2 z = \int_0^z \int_0^{2\pi} \left(\frac{R_1 + a_n e^{i(k_n z + n\theta)}}{2} \right)^2 d\theta\, dz$$

Integrating this gives

$$R_o^2 = R_1^2 + \left(\frac{a_n}{2}\right)^2$$

or

$$R_o = R_i \quad \text{to first order in } \frac{a_n}{R_o} .$$

I shall now calculate the increase in potential energy per unit length of the jet due to the surface deformation

$$(2) \qquad r = R_o + a_n e^{i(k_n z + n\theta)}$$

The increase in potential energy is assumed to be strictly due to the surface tension acting on the jet.

A short integration yields that the surface area per unit length of the jet is

$$s = 2\pi R_o + \frac{\pi}{4R_o}\left(k_n^2 R_o^2 + n^2 - 1\right) a_n^2$$

Therefore the change in potential energy due to the deformation is

$$(3) \qquad \Delta P = \frac{\pi}{4R_o} T \left(k_n^2 R_o^2 + n^2 - 1\right) a_n^2$$

For n positive, it is seen that this increase is always positive, giving us that the motion of the surface is damped. This is to say, all non-axisymmetric perturbations on the system are damped away.

For n identically zero, stability is achieved for

$$k^2 R_o^2 > 1$$

The system is unstable when $\Delta P < 0$ which is just

$$(4) \quad k^2 R_o^2 < 1$$

or

$$\lambda > 2\pi R_o$$

To calculate the dispersion relation for the simple capillary instability, it remains to calculate the kinetic energy of the jet. A Lagrangian for the system will then be defined, and the dispersion relation will be obtained by substituting this into Lagrange's differential equations of motion.

Since instability is achieved for n = 0 (equation 2), the dispersion relation will only be calculated for this.

To calculate the kinetic energy ΔKE, the velocity function for the column must be known. This is most easily obtained by finding the velocity potential

for the motion. The velocity potential Φ satisfies the following equations.

$$(5) \quad \underline{v} = \nabla \Phi \; ; \quad \nabla^2 \Phi = 0$$

The function which satisfies this and the surface condition given be equation 2 is (I_o is a Bessel function)

$$\Phi = A\, I_o(kr) \cos kz$$

The coefficient A is given when one equates the normal velocity at the surface with $\dot{r}$ at the surface. This gives that

$$A = \frac{\dot{a}_o}{kR_o\, I_o'(kR_o)}$$

Thus since the kinetic energy ΔKE is given by

$$\Delta KE = \tfrac{1}{2}\rho \int 2\pi R_o \Phi \left.\frac{d\Phi}{dr}\right|_{r=R_o} dz \qquad (7, \text{ p185})$$

we have that

$$(6) \quad \Delta KE = \tfrac{1}{2}\rho \pi R_o^2 \frac{I_o(kR_o)}{kR_o I_o'(kR_o)} \dot{a}_o^2$$

This enables us to define the Lagrangian L of the system by

$$L = \Delta KE - \Delta P$$

or

$$L = \frac{\pi}{2}\left[\rho R_o^2 \frac{I_o(kR_o)}{kR_o I_o'(kR_o)} \dot{a}_o^2 - \frac{T}{R_o}(1 - k^2 R_o^2)\, a_o^2\right]$$

From Lagrange's method

$$\Delta \int_{t_o}^{t_1} L \, dt = 0$$

giving us that

$$\dot{a}_o^2 + \omega^2 a_o^2 = 0$$

so that

$$a_o = a_o(0)\, e^{\omega t}$$

where

$$(7) \quad \omega^2 = \frac{T}{\rho R_o^3} \frac{kR_o I_o'(kR_o)}{I_o(kR_o)} (1 - k^2 R_o^2)$$

This is the dispersion relation for the unstable capillary jet.

A slightly more general analysis for arbitrary mode has the dispersion relation for the n th mode is

$$\omega_n^2 = \frac{T\, I_n'(x)\, x}{\rho\, R_o^3\, I_n(x)} (1 - n^2 - x^2)$$

where

$$x = k R_o$$

For $n > 0$, ω_n is imaginary for all x and n. For these modes, the waves do not grow in time. Thus the system is stable for all modes $n > 0$ which implies that the jet is stable for all non-axisymmetric disturbances.

The Sausage Instability

The sausage instability is the name given to the unstable n = 0 mode. As stated before, the growth rate for this mode is

$$\omega_o^2 = \frac{T}{\rho R_o^3} \frac{x(1-x^2) I_o'(x)}{I_o(x)}$$

where

$$x = k R_o$$

Also, as seen before, this mode is only unstable when

$$0 < x < 1$$

or

$$\lambda > 2\pi R_o$$

A plot of this dispersion relation is shown in Graph 1. It shows that the maximum growth rate occurs when

$$k = 0.697 \; R_o^{-1}$$

In any jet vibrating at random, this is the wavenumber that will dominate. For consider a surface made up of all the different growing waves

$$e^{\omega_1 t}, \; e^{\omega_2 t}, \ldots$$

After a time t the term which will dominate will have ω as a maximum.

GRAPH 1

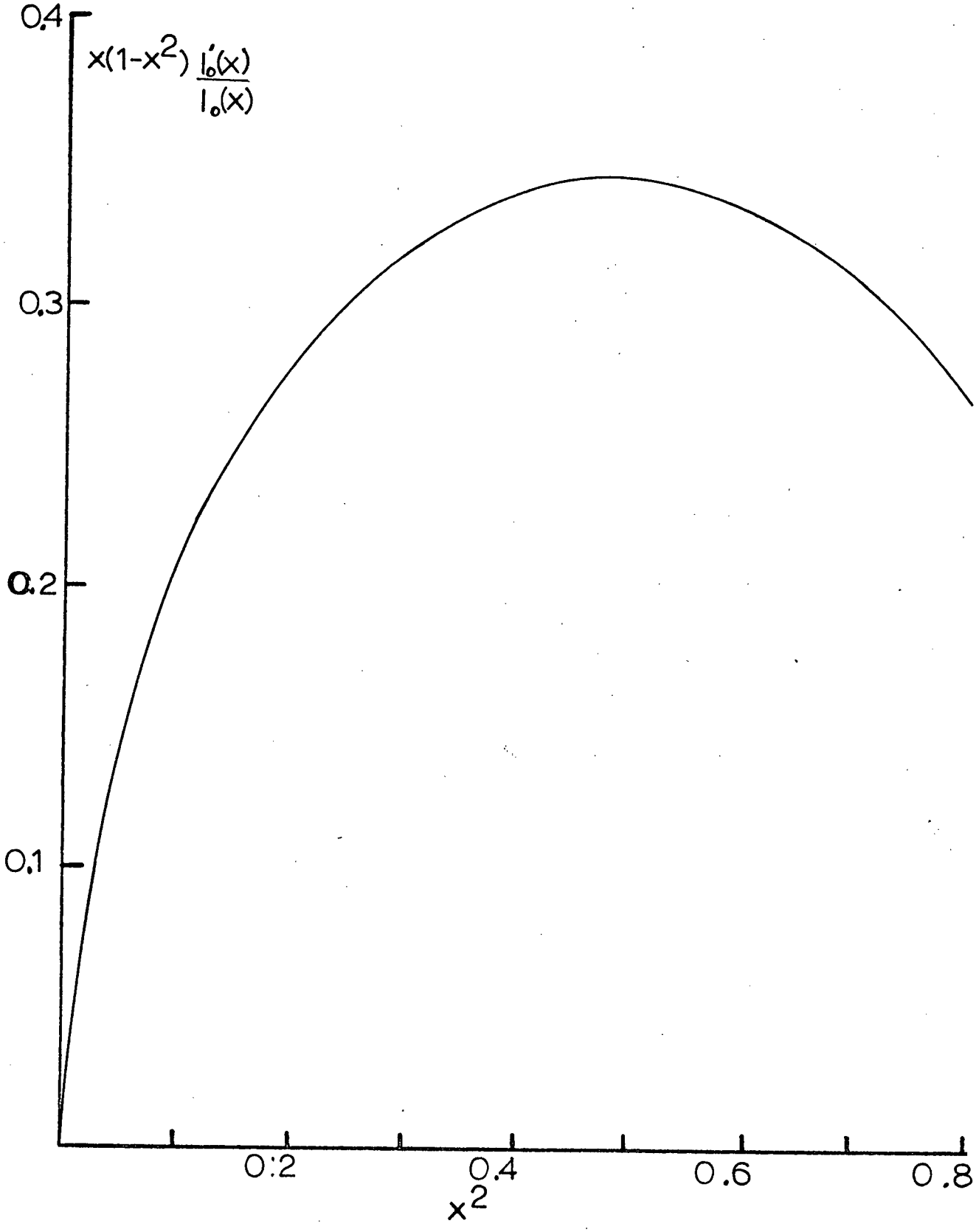

$x(1-x^2)\frac{I_0'(x)}{I_0(x)}$ vs. x^2

The M.H.D. Equations

Magnetohydrodynamics (M.H.D.) is essentially the study of the motions of electrically conducting fluids acting under the influence of magnetic fields. The term fluid is used so that the medium can be treated as a continuum; ie. all parameters of interest are taken as an average over a macroscopic interval large enough to remove the microscopic variations in the parameter, yet small in comparison to the fluid as a whole.

Consider a conducting fluid in an external magnetic field. The e.m. fields that are present are then this external magnetic field plus an electromagnetic field due to motion of the fluid.

Let:
- ρ be the density of the fluid
- σ be the conductivity of the fluid.
- ν be the viscosity of the fluid.
- $\underline{V}$ be the fluid velocity.
- p be the fluid pressure.
- $\underline{E}$ be the electric field strength.
- $\underline{H}$ be the magnetic field intensity.
- $\underline{J}$ be the current density.

The rationalized M.K.S. system of units is to be used.

The fluid nature of the flow is governed by the continuity equation and the Navier-Stokes equation with the forces due to the e.m. fields present. The e.m. fields are governed by Maxwell's equations, or equations directly derivable from them.

The following equations govern an M.H.D. flow for a fluid of constant viscosity.

$$\text{(8-1)}\quad \text{curl}\ \underline{E} = -\mu_o \frac{\partial \underline{H}}{\partial t}$$

$$\text{(8-2)}\quad \text{curl}\ \underline{H} = \underline{J}$$

$$\text{(8-3)}\quad \text{div}\ \underline{H} = 0$$

$$\text{(8-4)}\quad \text{div}\ \underline{J} = 0$$

$$\text{(8-5)}\quad \underline{J} = \sigma(\underline{E} + \mu_o \underline{V} \times \underline{H})$$

$$\text{(8-6)}\quad \frac{\partial \rho}{\partial t} + \rho\, \text{div}\ \underline{V} = 0$$

$$\text{(8-7)}\quad \frac{\partial \underline{V}}{\partial t} + (\underline{V}\cdot\nabla)\underline{V} = \frac{1}{\rho}\left[-\nabla p + \mu \underline{J} \times \underline{H}\right] + \nu \nabla^2 \underline{V} + \frac{1}{3}\nu \nabla(\nabla \cdot$$

These equations are valid under the following conditions.

- continuous fluid of constant viscosity.
- constant temperature throughout the fluid.
- characteristic frequencies are low.
- Hall effect and displacement currents are neglected.
- electric force is negligible in comparison with $\underline{J}\times\underline{B}$ force due to external magnetic fields.
- current generated by gradients in temperature, pressure, and density is neglected in comparison with currents generated by e.m. fields.

No derivation or justification will be given for these equations for it can be found in most standard textbooks on M.H.D. phenomena (12).

These equations shall be used when discussing the unstable jet with an axial current flowing down it. Only axisymmetric perturbations will be considered. That is, I will only consider the sausage instability mode. The form of the surface perturbation will be taken to be

$$a \cos kz.$$

The Unstable Jet with Axial Current (The Sausage Mode)

Again, let us consider a long cylinder of conducting fluid, but now, let a current I flow down the column. As in the case of the capillary jet, neglect the effects of gravity.

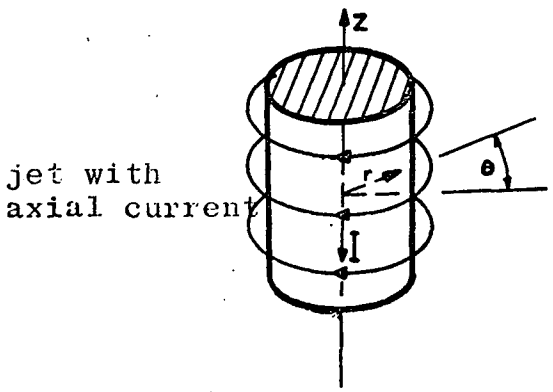

FIG 2-3

The current I produces a circular magnetic field $\underline{H}_o$ about the column.

It again can be seen qualitatively that such a situation is unstable. In addition to surface tension, the column is further constricted by the magnetic field. The force 'squeezing' the column goes as $I \cdot \underline{H}$ and $\underline{H}_o$ goes as R^{-1} so that if R is reduced, the force increases.

Pictorially, one can see two types of instabilities arising (see Fig. 2-4.).

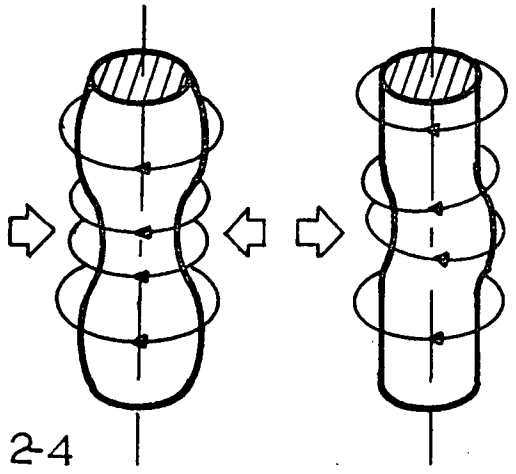

FIG. 2-4

sausage and kink instabilities

Before the jet is disturbed an any way, we have the equilibrium state as shown in Fig 2-3. The equilibrium current density J_o is given by

$$J_o = \frac{-I}{\pi R_o^2} \hat{k} \qquad r \leq R_o$$

where $\hat{k}$ is the unit vector in the z direction. The material outside the jet is assumed to be a vacuum so that $\underline{J} = 0$ outside the jet.

One then has that the undisturbed magnetic field is strictly toroidal, and is given by

$$H_o = (0, H_\theta, 0)$$

where

$$H_\theta = \begin{cases} \frac{J_o r}{2} & r \leq R_o \\ \frac{J_o R_o^2}{2r} & r \geq R_o \end{cases}$$

where matching has been done at $r = R_o$.

Let us now investigate the stability of the jet by calculating the change in potential energy as a result of an axisymmetric deformation to our column of the type given by equation 2 with n = 0.
The potential energy is the sum of the surface tension energy and the energy associated with the magnetic field.

Consider first, the change in surface tension energy ΔS_T as a result of the deformation. As before

$$\Delta S_T = \frac{T}{4 R_o}(k^2 R_o^2 - 1)\, a^2$$

This term will not change with the addition of an axial current if we make the assumption that the surface tension does not depend on the current flowing through the jet.

The change in magnetic energy as a result of a deformation to the surface is not so easy to calculate. This change can be calculated by finding the work done in perturbing the jet against the Lorentz force

$$\mu_o \underline{J} \times \underline{H}$$

If we displace the surface from $\underline{\xi}$ to $\underline{\xi} + \delta\underline{\xi}$, the change in magnetic energy as a result of the deformation is

$$M = -\frac{2\pi}{L} \int_0^L \int_0^a \int_{R_o}^{R_o + a\cos kz} \delta\underline{\xi} \cdot \underline{J} \times \underline{H}\, r\, dr\, dz$$

Now let us find the magnetic field and current density after we have perturbed the surface of the jet. These can be found to first order by a perturbation expansion:

$$\underline{H} = \underline{H}_o + \underline{h}$$
$$\underline{J} = \underline{J}_o + \underline{j}$$
$$\underline{V} = \underline{V}$$

The governing equation for $\underline{H}$ and $\underline{J}$ is found from equations 8-1 and 8-5 from which

$$\frac{\partial \underline{H}}{\partial t} = - \nabla \times \left(\frac{\underline{J}}{\mu_o \sigma} + \underline{V} \times \underline{H} \right)$$

If we assume that σ is small then this equation reduces to

$$\nabla \times \underline{J} = 0$$

The solution of this which is compatible with the surface shape is

$$J_r = \frac{ik J_o I_o'(kr)}{I_o'(kR_o)} a e^{ikz}$$
$$J_\theta = 0$$
$$J_z = J_o - \frac{J_o k I_o(kr)}{I_o'(kR_o)} a e^{ikz}$$

We now have $\underline{J}$ so that the only remaining calculation before we can evaluate the magnetic energy is the finding of the magnetic field resulting from the perturbation.

The magnetic field which corresponds to this current density

$$H_r = 0 = H_z \qquad \text{inside}$$
$$H_\theta = \frac{J_o r}{2} - J_o \frac{I_o(kr)}{I_o'(kR_o)} a e^{ikz} \qquad \text{the jet}$$

$$H_r = 0 = H_z \qquad \text{outside}$$
$$H_o = \frac{J_o R_o^2}{2r} \qquad \text{the jet}$$

Using these to evaluate the magnetic energy we get

$$(9) \quad M = \frac{\pi i}{4} \mu_o J_o^2 R_o^2 \left(\frac{I_o(kR_o) I_2(kR_o)}{I_1^2(kR_o)} - 1 \right) a^2$$

This calculation is just long and tedious so will not be given here (14).

This gives us that the potential energy change as a result of the surface deformation is

$$(10) \quad \Delta P = \frac{\pi T}{4 R_o} (k^2 R_o^2 - 1) a^2$$
$$\Rightarrow \frac{\pi}{4} \mu_o J_o^2 R_o^2 \left(1 - \frac{I_o(kR_o) I_2(kR_o)}{I_1^2(kR_o)}\right) a^2$$

Instability occurs when ΔP is negative, which is just

$$k^2 R_o^2 < 1 + \frac{J_o^2 R_o^3 \mu_o}{T} \left(1 - \frac{I_o(kR_o) I_2(kR_o)}{I_1^2(kR_o)}\right)$$

It is seen that the jet is unstable over a greater range of wavelengths as compared to the case of surface tension alone.

To get the dispersion relation for the jet, one needs to see how this potential energy is dumped into the kinetic energy of the flow, The kinetic energy of the flow has been calculated before (equation 6).

We can now define a Lagrangian for the system as

$$L = \Delta KE - \Delta P$$

If we then substitute this into Lagrange's equation

$$\Delta \int_{t_0}^{t_1} L \, dt = 0$$

it is apparent that

$$a(t) = a(0)\, e^{\pm \omega t}$$

where

$$(11) \quad \omega^2 = \frac{T x(x^2-1) I_1(x)}{\rho R_0^3 \, I_0(x)} + \frac{\mu_0 I^2}{2\pi^2 \rho R_0^4}\left(\frac{I_2(x)}{I_1(x)} - \frac{I_1(x)}{I_0(x)}\right)$$

A plot of this dispersion relation for a jet of radius 0.136 cm. composed of mercury with surface tension 487 dynes/cm. and density 13.6 g/cm. is shown in Graph 2. The graph only shows the unstable portion of the dispersion relation. It is seen that the growth rate increases approximately linearly with current (see Graph 2). It is also seen that the wavenumber of maximum instability increases with current.

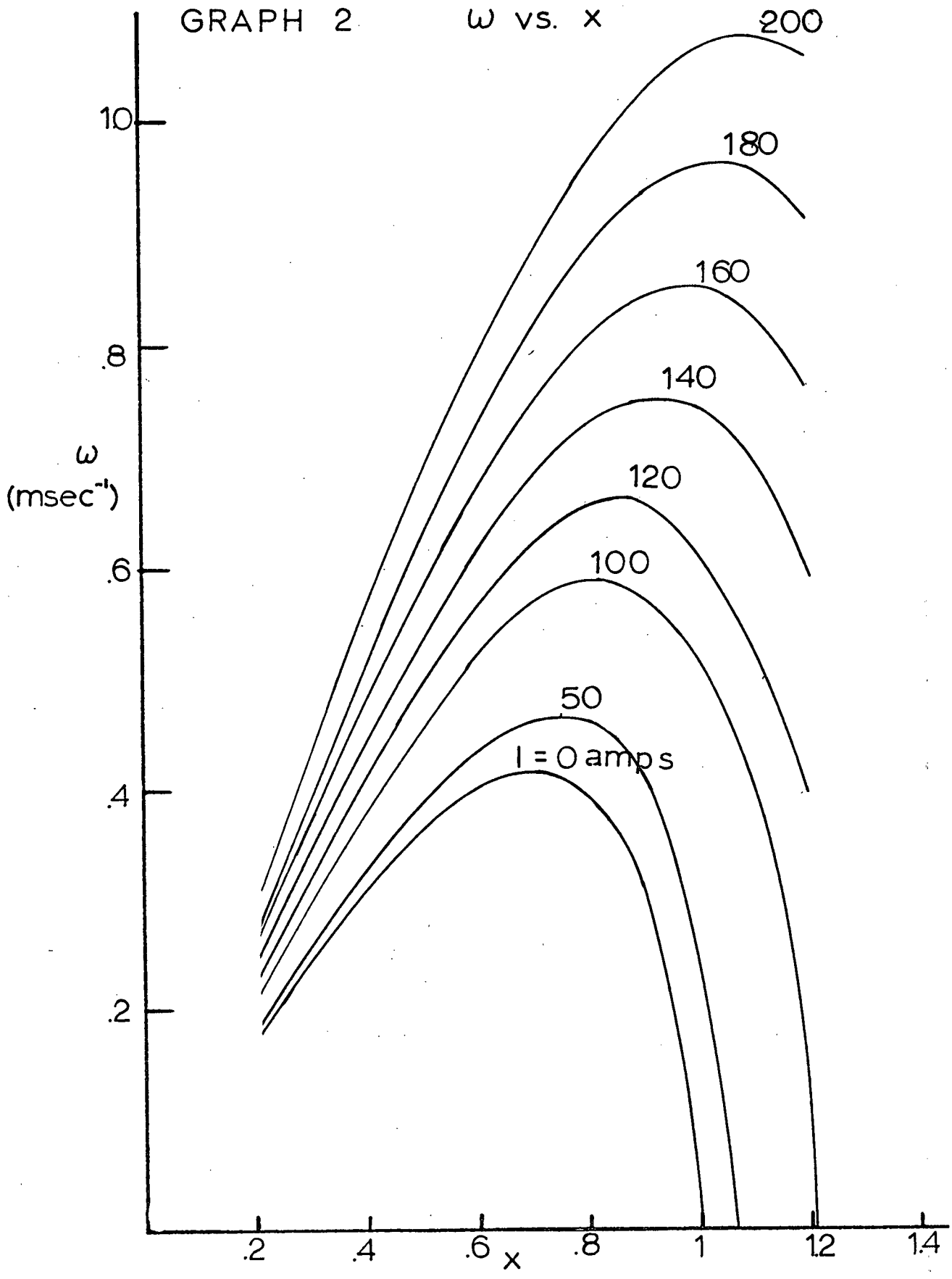
GRAPH 2
ω vs. x
200
180
160
140
120
100
50
I = 0 amps
10
.8
.6
.4
.2
ω
(msec⁻¹)
.2
.4
.6
.8
1
1.2
1.4
x

Velocity Effects

It will be seen in chapter 4 that it was necessary to allow the jet to flow down a notched central rod to achieve the proper surface deformation. It will be seen in chapter 5 that in this situation, pinching of the jet proceeded first at an exponential rate, but then stopped, and the jet entered a new stable mode of existence. I shall now present a simple theory which accounts for this observed behavior.

Consider the pinching jet as shown in Fig. 2-5.

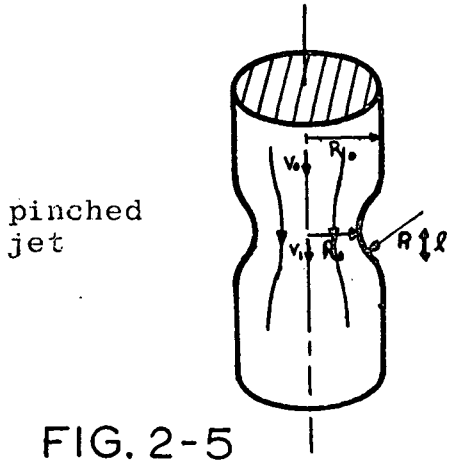

FIG. 2-5

The pinch is assumed to be held stationary in one position, while the jet flows through it. One can view the situation as a cylinder of taut wires to which an axial compression is applied. Squeezing forces are eventually balanced with a resistive force from the wires. Similarly for the flow, current and surface tension forces must fight to compress

the streamlines of the flow. Eventually an equilibrium is reached where the inward directed forces can no longer compress the streamlines.

To analyze the situation, we assume that the largest force driving the fluid over the shoulders of the depression is the magnetic pinching force. This force must balance the centrifugal force along a given streamline.

The centrifugal force scales as $\rho \frac{v_r^2}{R}$

where R is the radius of curvature of the surface near the shoulder of the pinch. Now

$$\frac{1}{R} \simeq \frac{a}{l^2}$$

where l is the length of the shoulder, and a is the amplitude of the pinch. The centrifugal force is then

$$\rho \frac{v^2}{l^2} a$$

To reach an equilibrium, this force must balance the magnetic pinching force F_{mag} which is

$$(12) \quad F_{mag} = \underline{J} \times \underline{B} \simeq \frac{\mu_o I^2}{R_o^3}$$

Hence

$$(13) \quad \frac{a}{R_o} = \frac{\mu_o I^2}{\rho R_o^2 v^2} \left(\frac{Cl}{R_o}\right)^2$$

where C is some dimensionless constant who's origin is often accredited to Cook, a mythical physicist.

A simple order of magnitude calculation shows that we are justified in neglecting $\frac{T}{R_o}$ in the above equation. That is, for the jet used,

$T = 487$ dyne $cm.^{-1}$

$R_o = 1$ mm.

$I = 100$ amps

$= 13.6$ gm/ cm^3

so that we have in M.K.S. units

$$\tfrac{1}{2}\rho v^2 \simeq 10^4$$

$$\frac{\mu_o I^2}{4\pi R_o^2} \simeq 5 : 10^3$$

$$\frac{I}{R_o} \simeq 5 \cdot 10^2$$

According to the above simple model, it is seen that the final pinch amplitude scales as the axial current squared, and inversely as the velocity of the flow squared.

In summary we have that initially, any axisymmetric perturbation grows in an exponential manner. This is due to the increasing inward magnetic pressure as the pinch progresses. However, after the pinch has progressed some small amount, the magnetic pressure finds increasing difficulty in compressing the streamlines of the flow. Eventually an equilibrium is reached where the magnetic field cannot compress the streamlines any further.

This equilibrium is an effect strictly due to the fact that the perturbation does not move with the jet. It it were free to move with the jet, there would be no streamlines to compress, so that the jet could pinch itself off completely.

Chapter 3 The Resonant Cavity

Consider the following- a cylindrical microwave cavity has a coaxial conducting rod which is undergoing small changes in shape. ie.

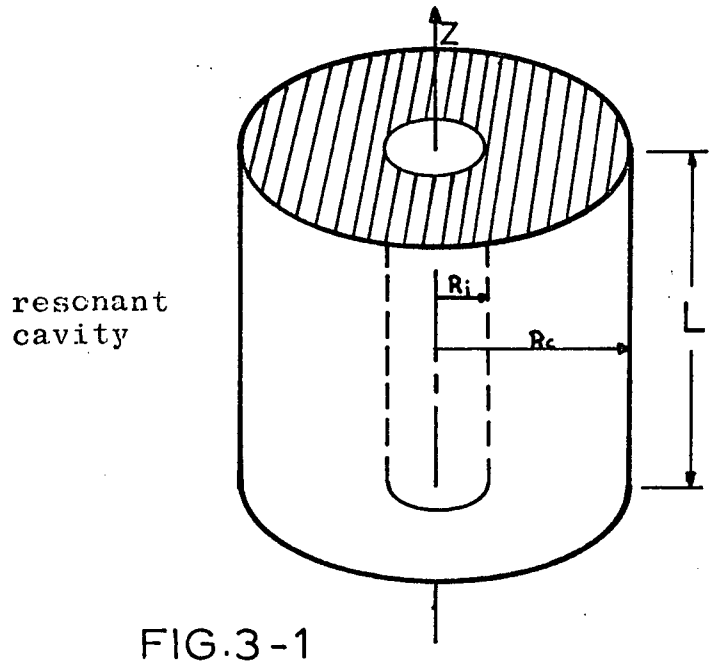

FIG.3-1

By studying the changes in the resonant frequency of such a cavity, one should be able to 'see' how the shape of the inner conductor is changing. This chapter gives a linearized account of how changes in R_i are linked to changes in the resonant frequency.

The attack to be used is the following; first the equilibrium configuration will be considered, ie. R_i is constant, and then small changes in R_i will be analyzed by a perturbation method centered around

"Slater's " theorem. (13)

The cavity shown in Fig 3-1 supports standing e.m. waves whenever

$$(14)\quad f = \frac{c}{2\pi}\left[\left(\frac{X_{lm}}{R_c}\right)^2 + \left(\frac{n\pi}{L}\right)^2\right]^{\frac{1}{2}}$$

where f is the excitation frequency of the microwaves entering the cavity and X_{lm} is a parameter given by the solution of the following equations.

TM modes $\quad J_l(X_{lm})\, N_l(\varepsilon X_{lm}) = J_l(\varepsilon X_{lm})\, N_l(X_{lm})$

TE modes $\quad J_l'(X_{lm})\, N_l'(\varepsilon X_{lm}) = J_l'(\varepsilon X_{lm})\, N_l'(X_{lm})$

where $\quad \varepsilon = \frac{R_i}{R_c}$

Since we want to detect changes in R_i , we want a resonant mode which depends heavily on ε . We also want a mode or series of modes which are not degenerate, ie. cavity configurations where single modes are present, not overlapping any other mode.

Modes which satisfy this property are the (0, 1, m) modes. For these modes, there are no radial currents in the end plates, and azimuthal changes in R_i do not appear.

Because no radial currents flow out of the end plates, we can insulate them from the cavity wall, thus allowing for the possibility of letting an external current flow down the coaxial column. The restriction of no azimuthal dependence allows only for the possibility of studying 'sausage' like changes on the inner conductor.

To calculate the shift in resonant frequency due to a perturbation on the inner conductor wall, we use "Slater's" theorem which is

$$f^2 - f_k^2 = \iiint (\underline{H}_k^2 - \underline{E}_k^2)\, dV \qquad (13)$$

where f_k is the resonant frequency for the unperturbed cavity in the k th mode with magnetic and electric fields $\underline{H}_k$ and $\underline{E}_k$ respectively. f is the resonant frequency of the cavity with the perturbation present. The volume integral is taken over that part of the cavity removed by the perturbation.

This has been done for the case of the TE_{omn} modes and is summarized in what follows. (2)

In the (0, m, n) modes there is no azimuthal dependence, so that the volume integral reduces to

$$2\pi \int_{R_i}^{R_i + \delta R_i} \int_0^L (\underline{H}_k^2 - \underline{E}_k^2)\, r\, dr\, dz$$

Further, $\underline{E}, \underline{H} \sim \cos \frac{n\pi}{L} z$

so that when we write the changes δR_i in the inner conductor's radius in a fourier series

$$\frac{\delta R_i}{R_c} = \Delta_o + \sum_1^\infty \left[\Delta_s \cos \frac{2\pi s}{L} z + b_s \sin \frac{2\pi s}{L} z \right]$$

with $\frac{\delta R_i}{R_c}$ assumed much smaller than $\frac{R_i}{R_c}$, the result of the integration to first order in $\delta R_i / R_c$ is

$$\frac{\delta f}{f_k} = (\Delta_o - \frac{\Delta_n}{2}) \, £$$

where

$$£ = £(\varepsilon, m, n, L, R_c) \qquad (6)$$

and

$$\delta f = f - f_k$$

This is cumbersome to say the least, and if the integral £ is to be tabulated in some reasonable manner, the whole expression needs to be put into dimensionless form. This has been done (6) with the result that

$$(15) \qquad \phi_{mn} \delta\phi_{mn} = \chi_m (\Delta_o - \frac{\Delta_n}{2})$$

where

$$\phi_{mn} = \frac{2\pi R_c}{c} f_{mn}$$

and

$$\chi_m = g(\varepsilon, m)$$

has been tabulated (ref. 6).

So it is immediately seen that for small changes in the radius of the inner conductor, monitoring the resonant frequency of some (0, m, n) mode gives the amplitude of the n th fourier component of the change in the radius of the inner conductor, that component having wavenumber $\frac{2\,n\,\pi}{L}$.

One then simply chooses a value of m which gives the desired sensitivity for looking at a particular fourier component.

Chapter 4 The Apparatus

The apparatus used to study surface instabilities on a liquid column is most conveniently described in three parts.

The first part is the hydraulic portion of the experiment in which the achievement of a relatively stable jet is described in detail. Some of the 'blind alleys' investigated will also be presented to help the future investigator to quicker success.

The microwave detection apparatus is now standard equipment in this laboratory. However, it will be described in some detail, along with the modifications made to it.

The third part ties together the rest of the apparatus. This consists of a discussion of the methods, both successful and unsuccessful, used to perturb the surface of the jet. The simple circuit used to pass an axial current down the jet will also be mentioned.

Hydraulic Portion

The hydraulic portion of the experiment as it now stands is the very simple arrangement shown in Fig. 4-1. Mercury flows from the upper reservoir, through a control valve, into a receiving chamber for the nozzle. The mercury flows from the nozzle, forming a jet which passes through a microwave cavity, and is collected in the bottom of the cavity. The mercury leaves the cavity and is collected in yet another reservoir from which it is transported back to the upper reservoir.

It is a well known fact that mercury is a very corrosive liquid (see appendix A-1). That is, it forms amalgams with most easily machined metals, and has a special affinity for brass and solder. This requires that if these sort of metals are to be used in the construction of the apparatus, they must be plated completely with some material that will not amalgamate with mercury. Nickel seems to be the most easily available and platable material. (see appendix A-2).

However, plating is not the final answer. Even on a well plated surface, especially near a corner, the nickel is highly stressed and eventually cracks, allowing mercury to attack whatever is beneath.

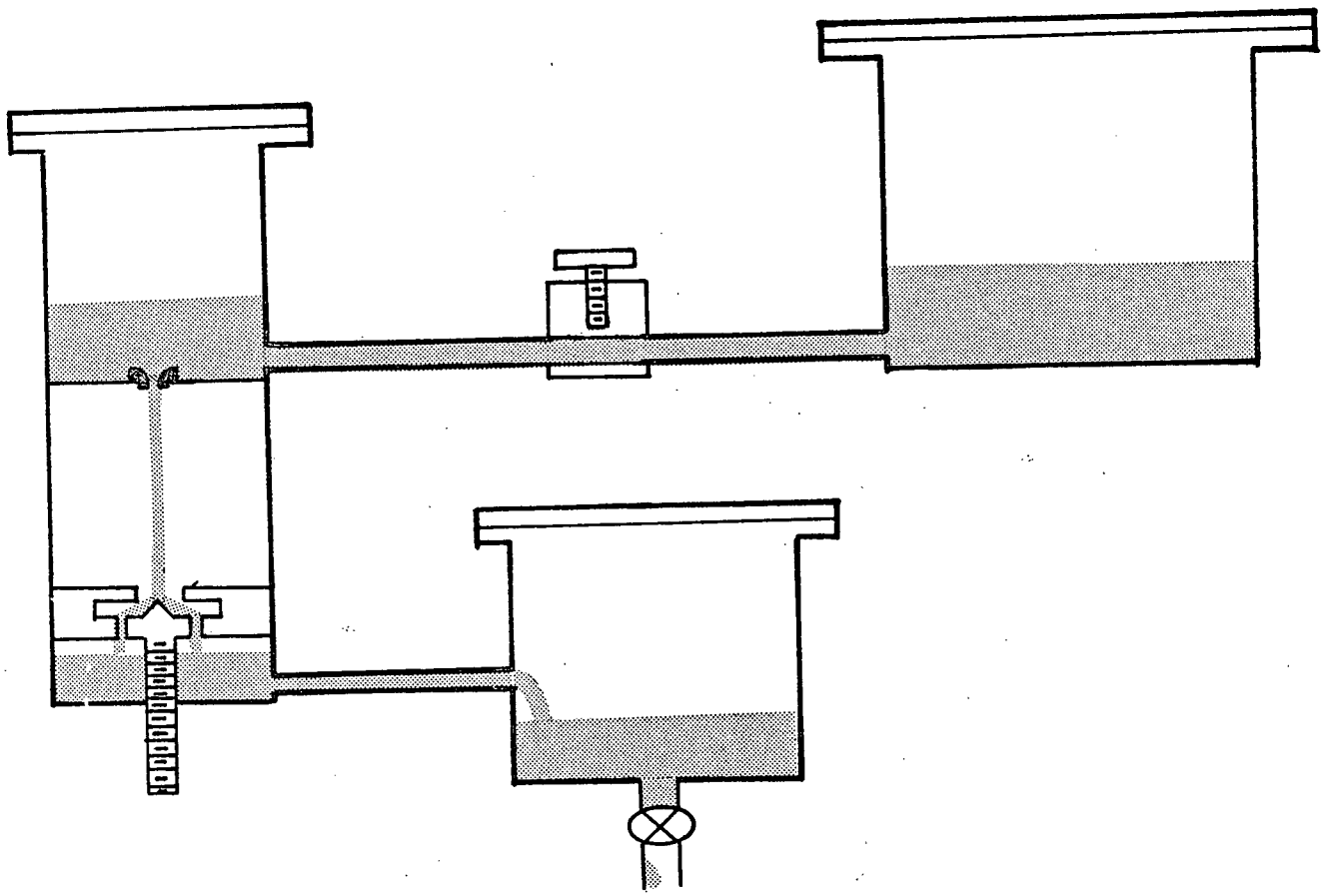

FIG. 4-1 The Hydraulic System

If it is a solder joint, a leak develops quickly. An unplated solder joint will leak in just a few hours if continually exposed to mercury. To prevent this, all joints were covered with epoxy. This provided a joint, which if not vibrated or twisted excessively, would last at least a year.

As was previously mentioned, the mercury flows from a nickel plated upper reservoir through a control valve, to the nozzle reservoir. The valve controls the volume flow of mercury which reaches the nozzle. It is a simple valve in which control in achieved by squeezing a short section of 'tygon' (polyvinyl chloride) tubing. This was chosen to avoid the corrosive action of mercury on valves other than those made of stainless steel.

We now have a controlled flow of mercury towards the nozzle. We have two adjustable parameters here- the nozzle diameter, and the mercury head above the nozzle. These must be adjusted to provide a 'convenient' observation time for a 'reasonable' volume of mercury.

The exit velocity of the jet, and the corresponding

flow rate can be determined from Torricelli's famous formula.* This states that

$$v = \sqrt{2gh}$$

where v is the exit velocity of the jet, g is the acceleration due to gravity, and h is the head of mercury above the nozzle. The fluid is inviscid and incompressible.

This gives a volume flow rate Q of

$$Q = \pi R_o^2 \sqrt{2gh}$$

where R_o is the radius of the jet at the nozzle exit.

* The derivation of Torricelli's formula is very simple from an energy standpoint. Consider the following

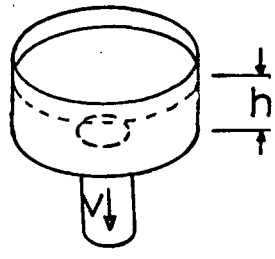

The energy of the system before the fluid element δV leaves the nozzle is just $\rho g h (V_{01})$. When the element leaves, the kinetic energy of the element $\frac{1}{2}\rho v^2 \delta V$. is equal to the potential energy $\rho g h \delta V$ lost so that

$$v^2 = 2gh$$

Thus a jet of 2 mm. diameter with a pressure head of 3 cm. Hg. has an exit velocity of about 77 cm/sec. and has a flow rate of 150 ml/min. or about 5 lb. of mercury per minute.

The nozzle and reservoir are shown in Fig 4-2.

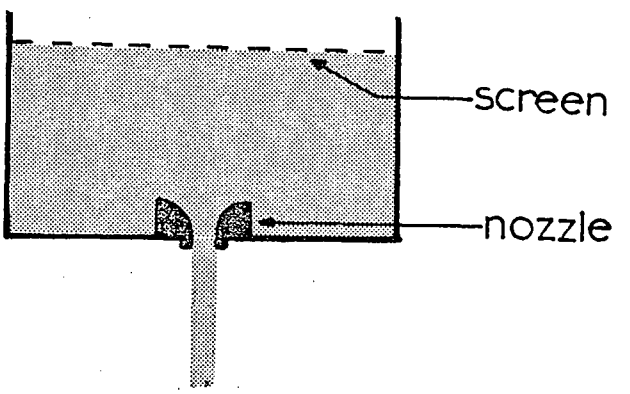

FIG. 4-2 nozzle and head

The screen, a brass mesh of 1/8 " spacing, prevents unwanted disturbances on the mercury head. It also eliminates the formation of a 'drain vortex' which would most certainly form otherwise, giving a rotation to tne jet.

According to boundary layer theory, most of the flow through an orfice flush with the bottom of the reservoir would come from the boundary layer

on the bottom of the reservoir and down the sides of the free vortex formed. By elevating the nozzle, the mercury is taken more uniformly from the reservoir. This provides a clean surface on the jet, free from the contaminants that may be in the bottom boundary layer and on the edge of the free vortex carried down from the surface.

It should be pointed out that a jet free of surface disturbances could not be achieved unless the nozzle was thoroughly wetted by the mercury. This meant that the nozzle, which was made of brass, had to be periodically washed in a dilute nitric acid solution to clean off surface oxidation.

It is well known that when a jet leaves a nozzle, it suffers a contraction as it falls. However, for the method of generating a controlled perturbation discussed later, it will be seen that this consideration is unnecessary.

The jet flows through a microwave cavity which analyzes any surface wave which may be present. This will be discussed later. It leaves the cavity by impinging on a brass needle which is thoroughly wetted with mercury. (see Fig. 4-3)

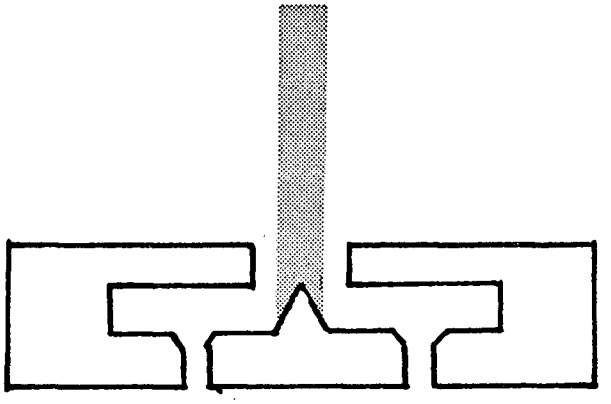

FIG. 4-3 collecting needle

This needle prevents the 'wandering' of the lower end of the jet and also reduces the vibrations sent back up the jet which are generated when the jet strikes a solid surface. Plates above the needle shield the distortion of the jet from the microwave cavity.

The mercury then leaves the cavity, is collected in the lower reservoir, and is then returned to the upper reservoir manually.

I will now mention a few modifications to the apparatus which were abandoned, as unnecessary.

The first type of flow system considered, is shown in Fig. 4-4.

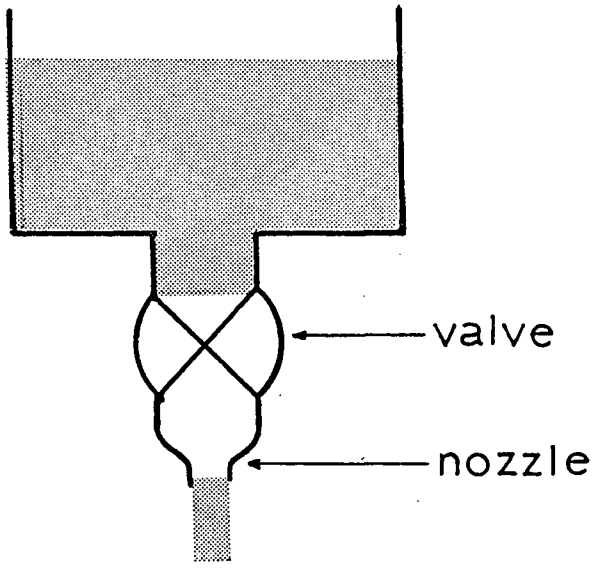

FIG. 4-4

original system

As can be seen from Fig. 4-4, a valve between the head and the nozzle was used to control the flow rate of mercury. This technique could never be made to work properly. Cavitation and turbulence generated behind the valve destroyed the stability of the jet.

A constant pressure head device was also constructed. It was not incorporated into the present system because the measurements are not yet sophisticated enough to warrant it. Besides, a solder joint in it, which was nickel plated, began to leak.

The constant head device was simply an overflow. When the mercury level above the nozzle got too high, the mercury flowed out of an overflow port and was drained into the lower reservoir, as is illustrated in Fig. 4-5.

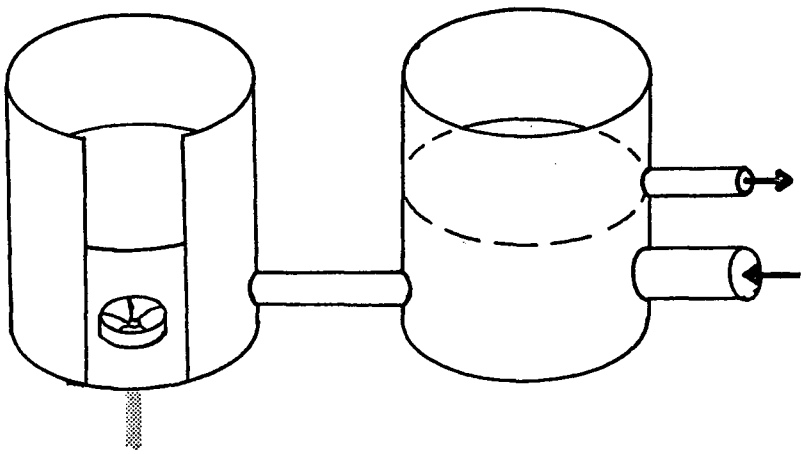

FIG. 4-5 constant head device

Although not necessary for the apparatus as it now stands, several methods of pumping the mercury from the lower reservoir to the upper reservoir were tried.

One such pump was a pneumatic pump. The lower

reservoir was sealed off from the rest of the system except for a return line to the upper reservoir. Air was forced into the lower reservoir at about 20 psi. above atmospheric pressure, and the mercury was forced up the return line. This method was not used because pouring the mercury by hand was easier and safer if the room was well ventilated.

A partially successful continuous pump was designed and built. This pump operated by the peristaltic squeezing of a rubber tube. However, it had one serious drawback. The rubber tubing used in the pump lasted for just a few hours before it cracked and allowed mercury to leak out. An acceptable tubing was not found, although manufacturers of this type of pump claim the polyvinyl chloride tubing with thin wall gives satisfactory preformance.

Microwave Portion

As mentioned previously, the microwave detection system is standard equipment in this laboratory and is described in sufficient detail elsewhere (3). I will here just summarize its function, and elaborate on any modifications made to the system. Fig.4-6 clearly illustrates the microwave equipment used.

The klystron (2K25) generates microwaves in the frequency range 8.6 to 9.6 k MHz. This is pin coupled to standard 3 cm. waveguide. An isolator prevents reflections from the rest of the system from interfering with the klystron's operation. The microwaves pass through a wavemeter, which is nothing more that a calibrated resonant cavity used to measure the frequency of the microwaves. This leads into a magic tee, one arm of which is terminated with an absorbing stub. The other arms go to a crystal detector and the cavity via a pin type impedance matcher.

The output of the klystron is modulated be placing the time base sawtooth of an oscilloscope on the reflector of the klystron. The entire frequency range is then swept through each time the scope traces once. This converts the horizontal axis

of the scope into a measure of the frequency. The output of the crystal detector goes to the vertical deflection of the scope. The oscillograms therefore give a measure of the power absorbed in the cavity as a function of the microwave frequency. The pattern seen of the scope is shown in Fig. 4-7.

It is seen that several operational modes of the klystron are displayed simultaneously. This means that the sawtooth voltage at the reflector is too great. A potentiometer was used to divide this voltage so that only one mode, or part of a mode, was displayed on the screen.

The detecting cavity is shown in Fig 4-10, the details of which will be given later. When the length L of the cavity is adjusted so that the cavity is in resonance with the incoming microwave signal,(cf. ch.3) the pattern displayed on the scope is as seen in Fig. 4-8 (see also Plate 1).

As was shown in chapter 3, a shift in the resonant frequency of the cavity in the n th cavity mode is proportional to the amplitude of the n th fourier component of a surface wave on the jet. Thus by watching the resonance move horizontally across the face of the scope, we get a measure of

the amplitude of the wave on the jet.

To record the shift of the resonant frequency in time, a simple smear camera was used. This is illustrated in Fig. 4-9. The camera consists of a polaroid camera back (Polaroid type 2620) pulled along by a spring, over the image of the oscilloscope screen on a standard oscilloscope camera. (Dumont 299)

The screen of the scope is masked off except for a horizontal line, as is shown in Fig, 4-8. In this way, only a dot is smeared along the film. The scope is triggered at a known rate, and the dot is displayed once every sweep of the trace. Thus a series of dots is displayed- each dot a certain known length of time apart. (see Plate 2) In this way, the nonlinearity of the motion of the camera back is not important.

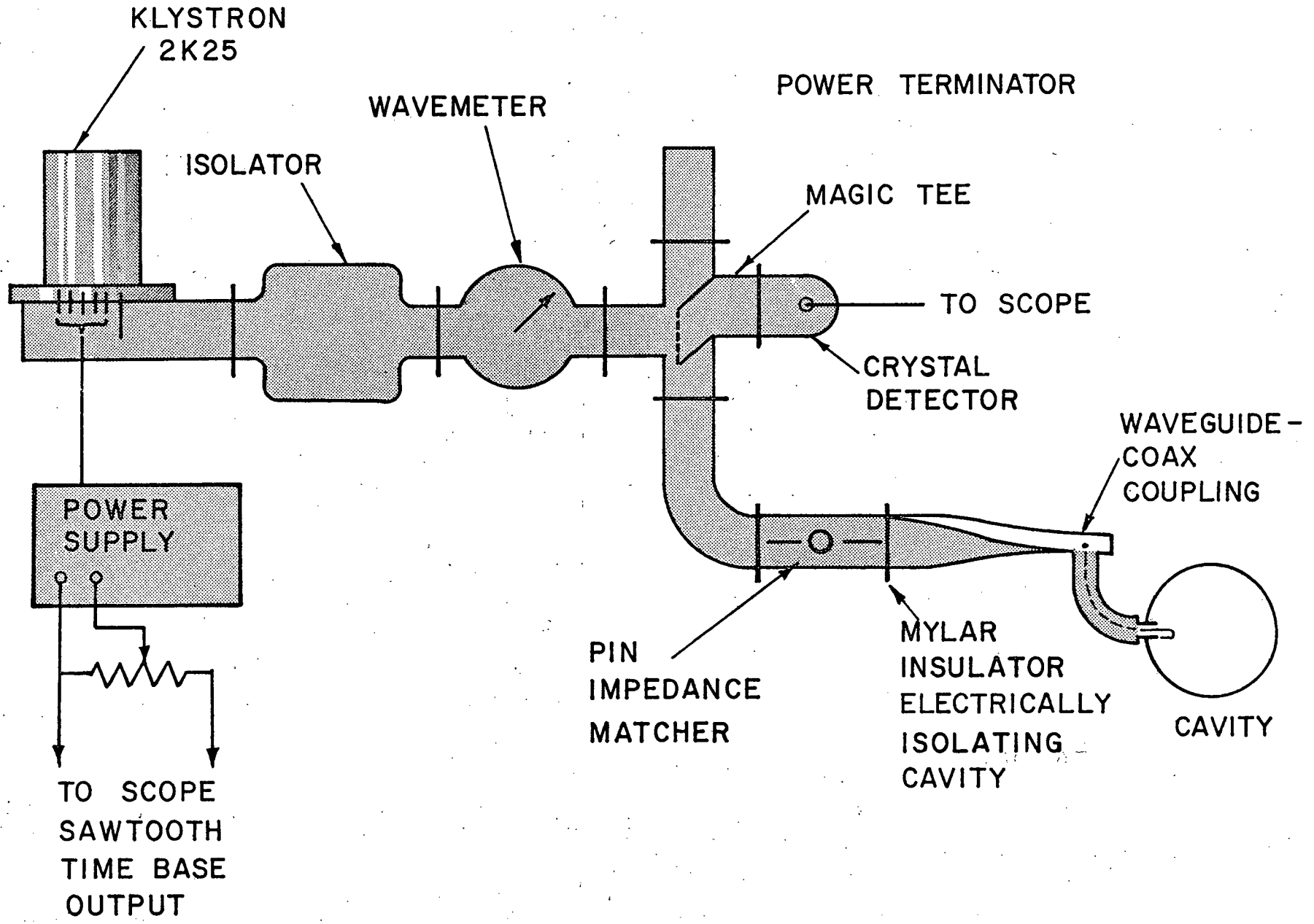

FIG. 4-6 Microwave Detection Apparatus

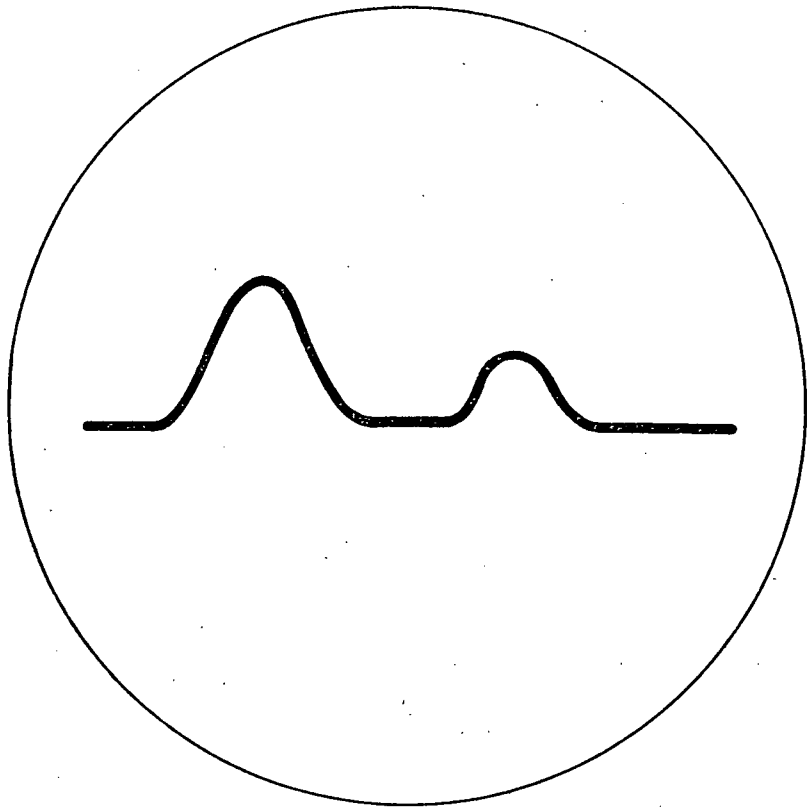

FIG. 4-7 Klystron Modes

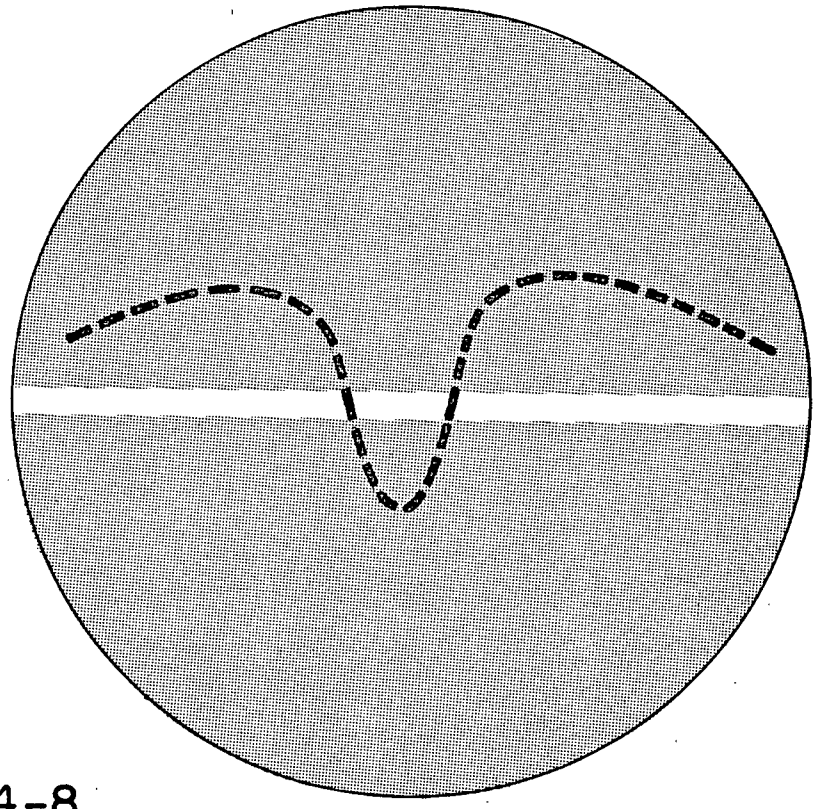

FIG. 4-8 The Mask

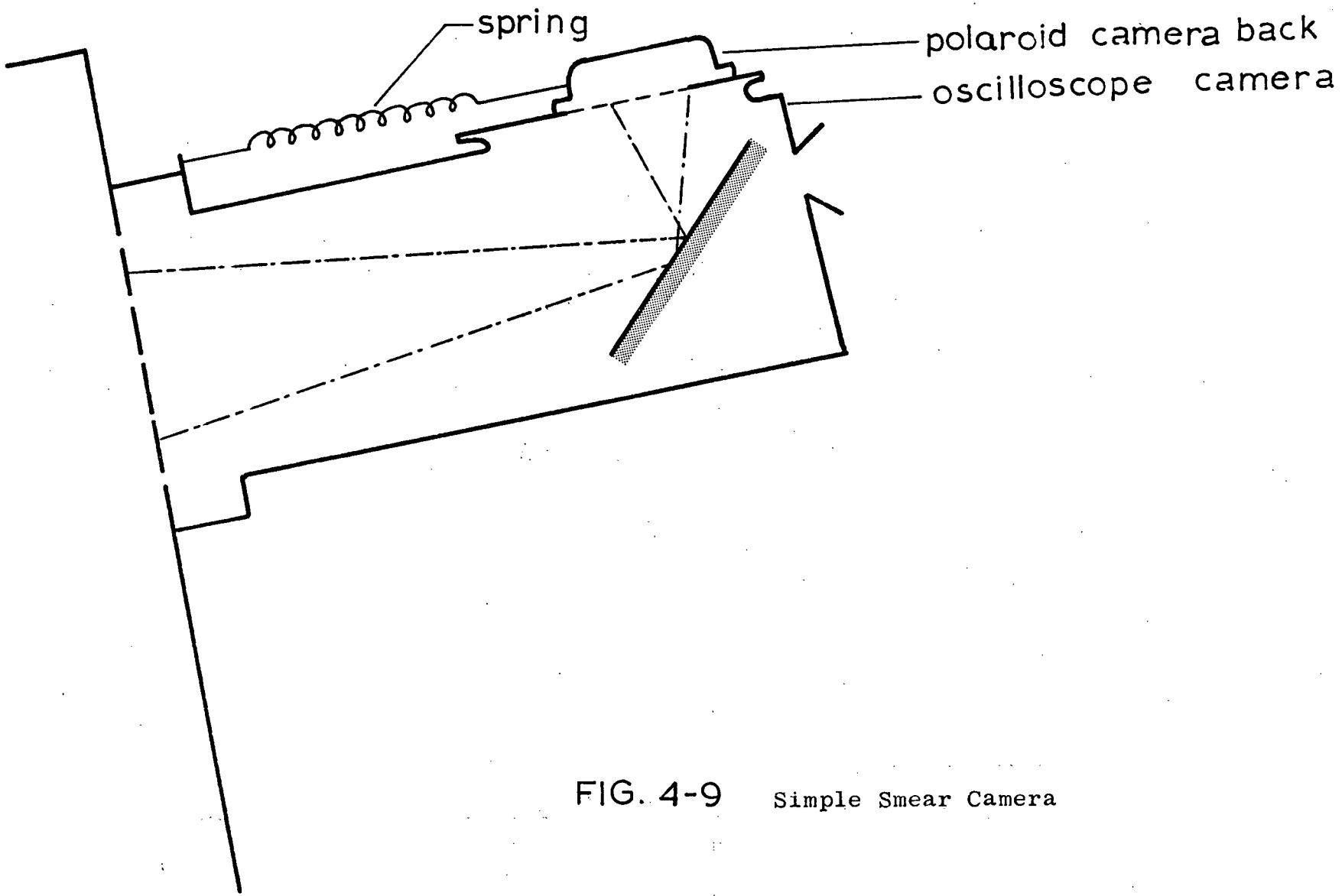

FIG. 4-9 Simple Smear Camera

The Cavity

The cavity is a nickel plated brass cylinder shown diagramatically in Fig. 4- 10. The microwaves enter the cavity via a loop through the side of the cavity. The nozzle reservoir for the jet is insulated from the sidewall of the cavity by a thin sheet of mylar. This serves two purposes. It permits all the current used to make the jet unstable pass down the jet, and it also inhibits radial currents due to e.m. radiation in the cavity. This necessarily restricts the cavity to the (0, m, n) modes.

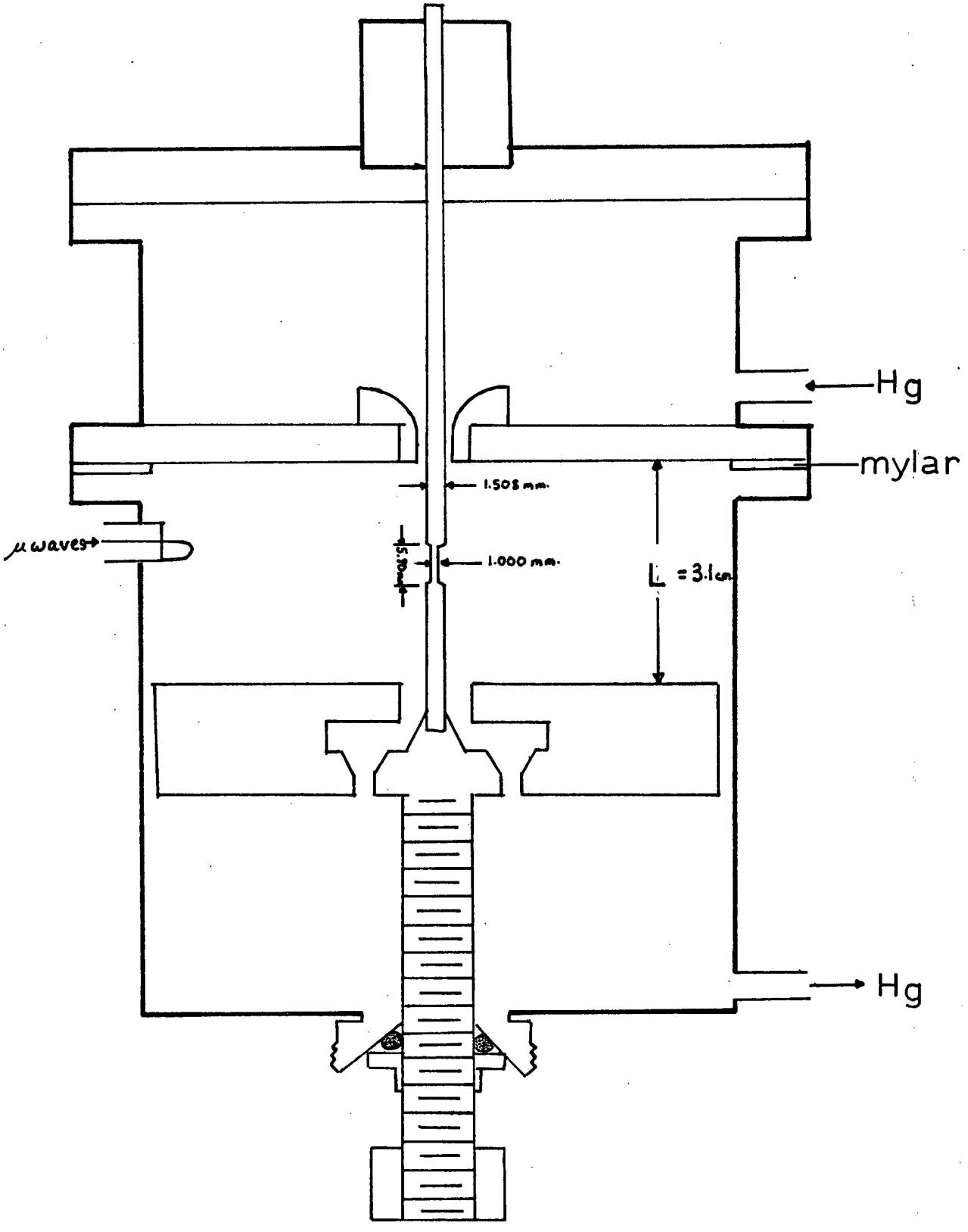

FIG. 4-10 Cavity Details

The Remainder

Once a stable mercury jet had been achieved, it remained to make it detectably unstable by some controllable perturbation to the surface. The desirable arrangement was to have a pure surface mode generated- a mode detected by the particular e.m. mode of the cavity used.

The final arrangement used, although not totally desirable, nevertheless worked. As can be seen from Fig. 4-11, the jet is forced to flow along the outside of a brass rod which is notched to create an indentation on the jet's surface.

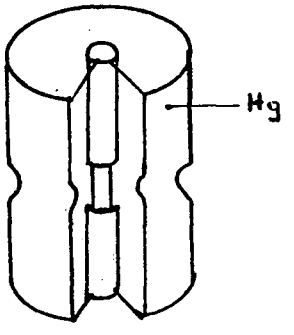

FIG. 4-11 Perturbation Generator

Of course, capillary instability is still present. Tnis shows up as an unwanted noise signal. (cf. ch. 4) A large axial current is now passed down the column through the arrangement shown in Fig 4-12.

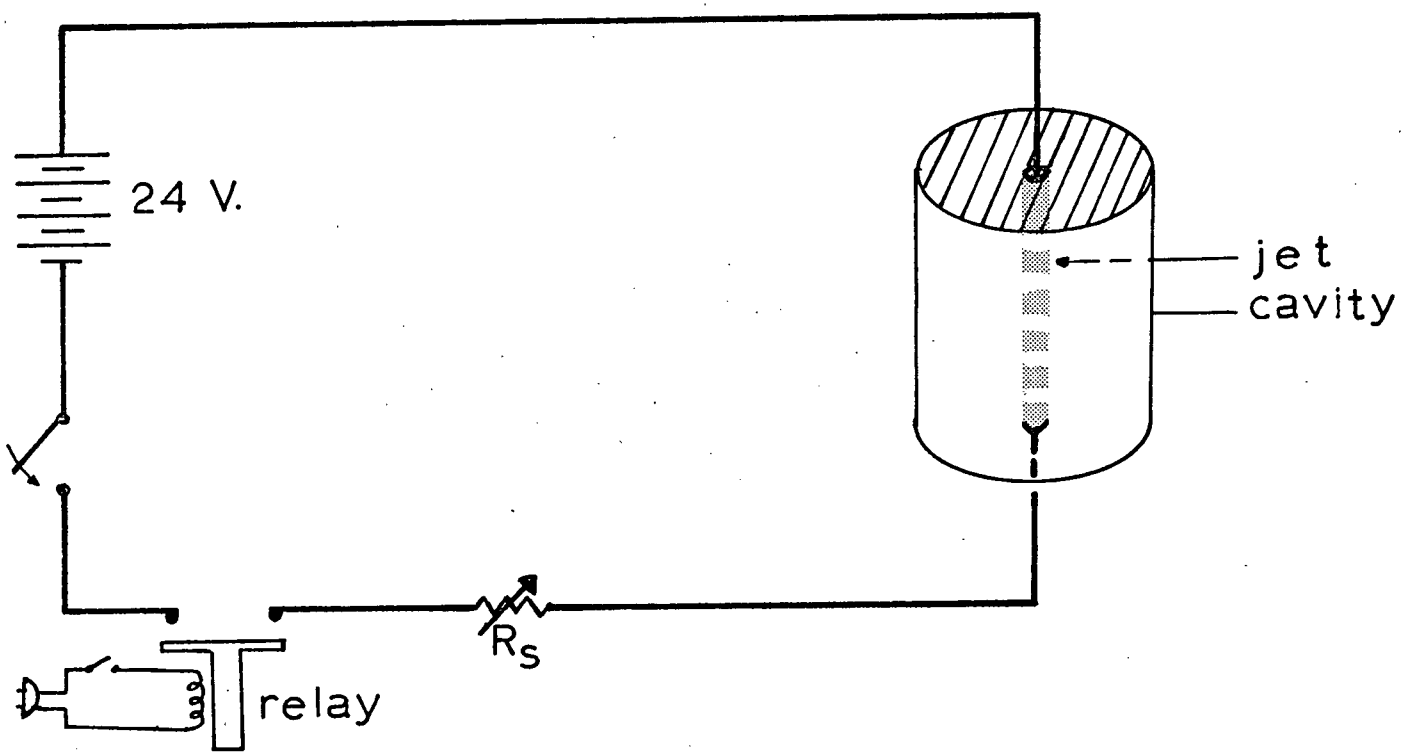

$$R_s = \frac{1}{n}\,\Omega \qquad n = 5,6,7,\ldots,12$$

FIG. 4-12 Supply for Axial Current

The self magnetic field pinches the jet at each notch in the central rod, thereby giving an unstable surface mode. The smear camera is released at approximately the same time that the relay is closed, and usually the instability is captured on film.

It was hoped that a workable alternative could be found for generating a controlled perturbation. A method which seemed hopeful is shown in Fig 4-13.

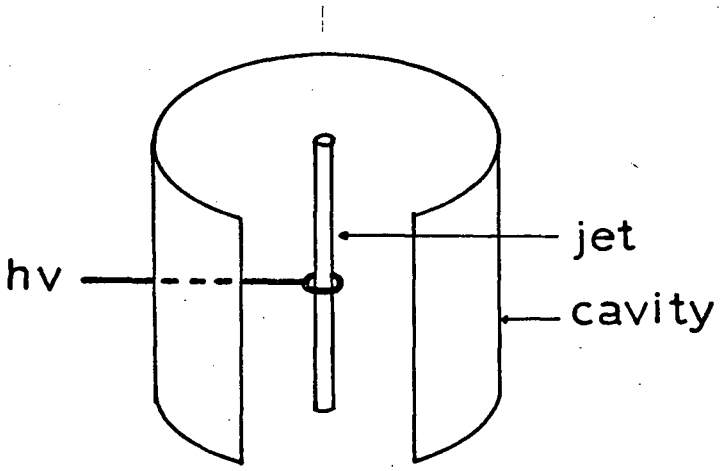

FIG. 4-13 Alternate Perturbation Source

The surface was to be stressed by the application of a high coaxial electric field at some point on the jet. The jet would be pulled out by a high voltage pulse (3), resulting in a controlled deformation to the surface. However, this method could not be made to work. No resonance with a large

enough Q could be found; the Q being destroyed by the distortion in the fields in the cavity by the high voltage lead-in wire.

Of course, one could design a cavity which would look at the mode of maximum instability which would most certainly dominate. However, the wavenumber of the most unstable mode changes with current, so separate cavities would have to be built for each value of current studied. This is clearly not feasible.

An attempt was made to generate a controllable perturbation by vibrating the jet with a loudspeaker driven by an audio oscillator. Needless to say, such a method did not work.

Chapter 5 The Results

To study the pinching of the jet with axial current, I needed to find a cavity resonance with a sharp Q. With only one notch in the wire, the mode would necessarily have to be the TE_{om1} mode. The resonance used is shown in Plate 1.

Referring to Fig. 4-10, the cavity resonance had the following properties:

$L = 3.05$ cm. $\pm$ 0.05 cm.

$R_i = 0.136$ cm. $\pm$ 0.003 cm.

$R_c = 4.28$ cm. $\pm$ 0.01 cm.

This means that the parameter $\varepsilon = \frac{R_i}{R_c}$ (cf. ch 2) is

$$\varepsilon = 0.0318 \pm 2\%$$

The klystron operating frequency was about 9.3 GHz. which when substituted into equation 14 gave that the mode used was TE_{021}. From (6) we then have, by graphical extrapolation

$$x_{02} = 7.053 \pm 2\% \quad \text{cm.} \qquad \text{eqn. 15}$$

Working backwards, and calculating the frequency from equation 14 puts the resonant frequency at

$f_o = 9.27 \times 10^9$ Hz. $\pm$ 2%

This corresponds well with the manufacturer's figure of 9.3 GHz.

As was stated earlier, we shall measure the size of the pinch by the change in the resonant frequency of the cavity. The change in resonant frequency was seen as a motion of the resonant dip across the oscilloscope screen. Thus, to relate this shift to the actual frequency change, a calibration curve is needed for the apparatus. Such a curve is given in Graph 3. The resonant dip was set to the middle of the scope screen, and so the shift is seen to be always in the linear portion of Graph 3 since the maximum amplitude was only of the order of 5 cm.

It can be seen from Graph 3 that a shift of one centimeter on the scope screen corresponds to a frequency change of 1.372 MHz.

We also need to know how much change in the shape of the inner conductor gives rise to a certain shift in the resonant frequency.

In equation 15, we have from (6) that

$$\chi_2 = 7.081 \pm 2\%$$

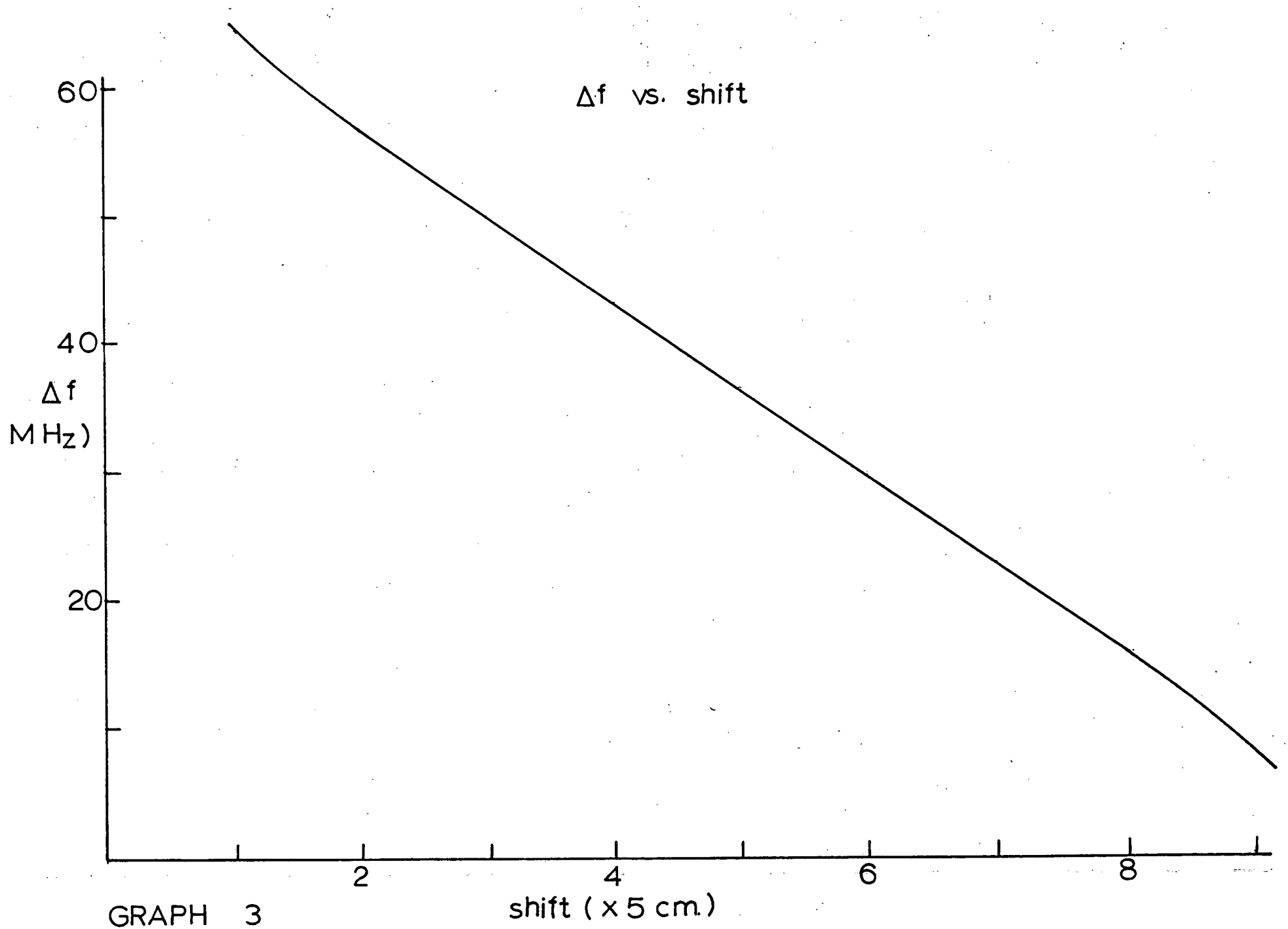

GRAPH 3

Now $\Delta_o = 0$ since there is assumed to be no overall compression to the jet. Then we have that

$$\Phi_{21} = 8.32 \pm 2\% \qquad \text{(cf. p. 33)}$$

and

$$\delta\Phi_{21} = 0.897 \times 10^{-9}\,\delta f$$

so that

$$\Phi_{21}\,\delta\Phi_{21} = 7.46 \times 10^{-9}\,\delta f \pm 2\%$$

but

$$\Phi_{21}\,\delta\Phi_{21} = 7.081\,\frac{\Delta_1}{2} \pm 2\%$$

so

$$\Delta_1 = 2.11 \times 10^{-9}\,\delta f \pm 4\%$$

Using the calibration fact that 1.372 MHz. change is registered as a one centimeter shift on the scope, we have the result that

$\Delta_1 = 2.89 \times 10^{-3}$ cm. change in the amplitude of a wave on the jet for every centimeter shift of the resonant dip on the scope. This is good to about $\pm$ 4%. That is to say, if the resonant frequency is lowered by one centimeter on the scope screen, the jet has pinched itself off 0.0289 mm. in the principal mode.

The instrument is now calibrated. The next step

was to look at the current generated instability. With the mercury flowing, the axial current was switched on, and the smear camera released simultaneously. The jet pinched itself off, and the shift in the resonant frequency was observed. A typical photograph of the event is shown in Plate 2.

Looking at Plate 2, it is seen that the jet before the instability is slightly noisy. This is the capillary instability growing and stopping when a given fluid element leaves the notch in the central rod.

When the current is switched on, it is seen that the jet pinches itself off very quickly. It should be noted that the time between dots on the photograph is 1.0 msec.

Because of the noisy nature of the signal, it was necessary to take several pictures at each value of axial current to get a truer value of the growth rate.

Now the disturbance on the surface of the jet is going to grow in general as

$$A e^{\omega t} + B e^{-\omega t}$$

However, at the instant the current is turned on, that is, at $t = t_o$, the surface is stationary.

This means that

$$a(t) = a(0) \cosh \omega(t - t_o)$$

However, the data is taken in the form

$$s = C \cosh \omega(t - t_o) + D$$

where s is the shift in centimeters of the resonance, D describes the arbitrary reference line from which the measurements were made.

If we expand $\cosh \omega (t - t_o)$, then for small $(t - t_o)$,

$$\cosh \omega(t - t_o) = 1 + \frac{\omega^2}{2}(t - t_o)^2$$

so that by plotting s against $(t - t_o)^2$, then initially the curve would be a straight line with slope

$$\frac{\omega^2}{2}$$

The analysis of Plate 2 is shown in Graphs 4 and 5. Graph 4 is just an expanded plot of Plate 2. Graph 5 shows the displacement against $(t - t_o)^2$. From this graph, the slope is seen to be 0.0776 giving

$$\omega = 0.394 \text{ msec.}^{-1}$$

The operating current was 170 amps.

GRAPH 4

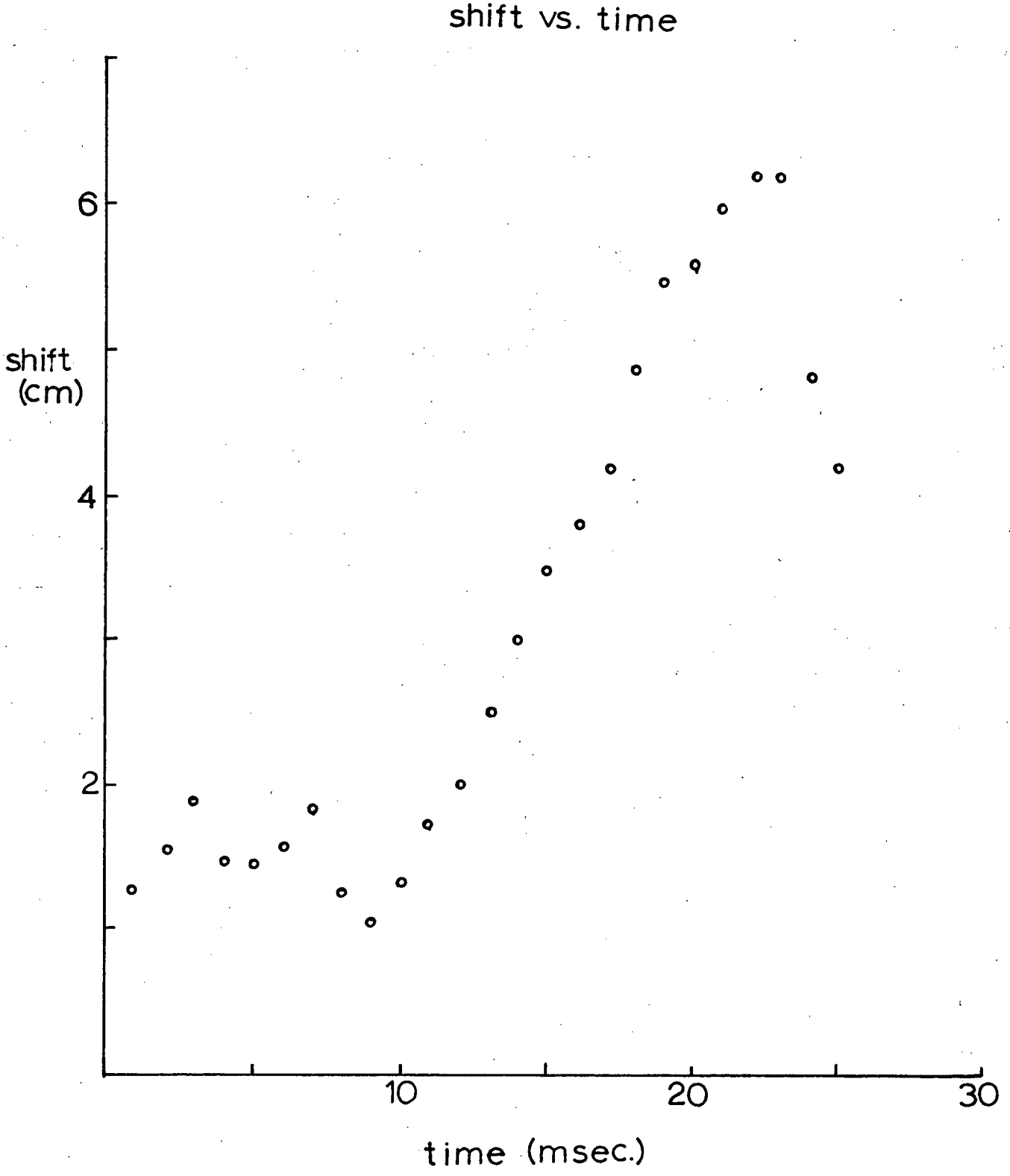

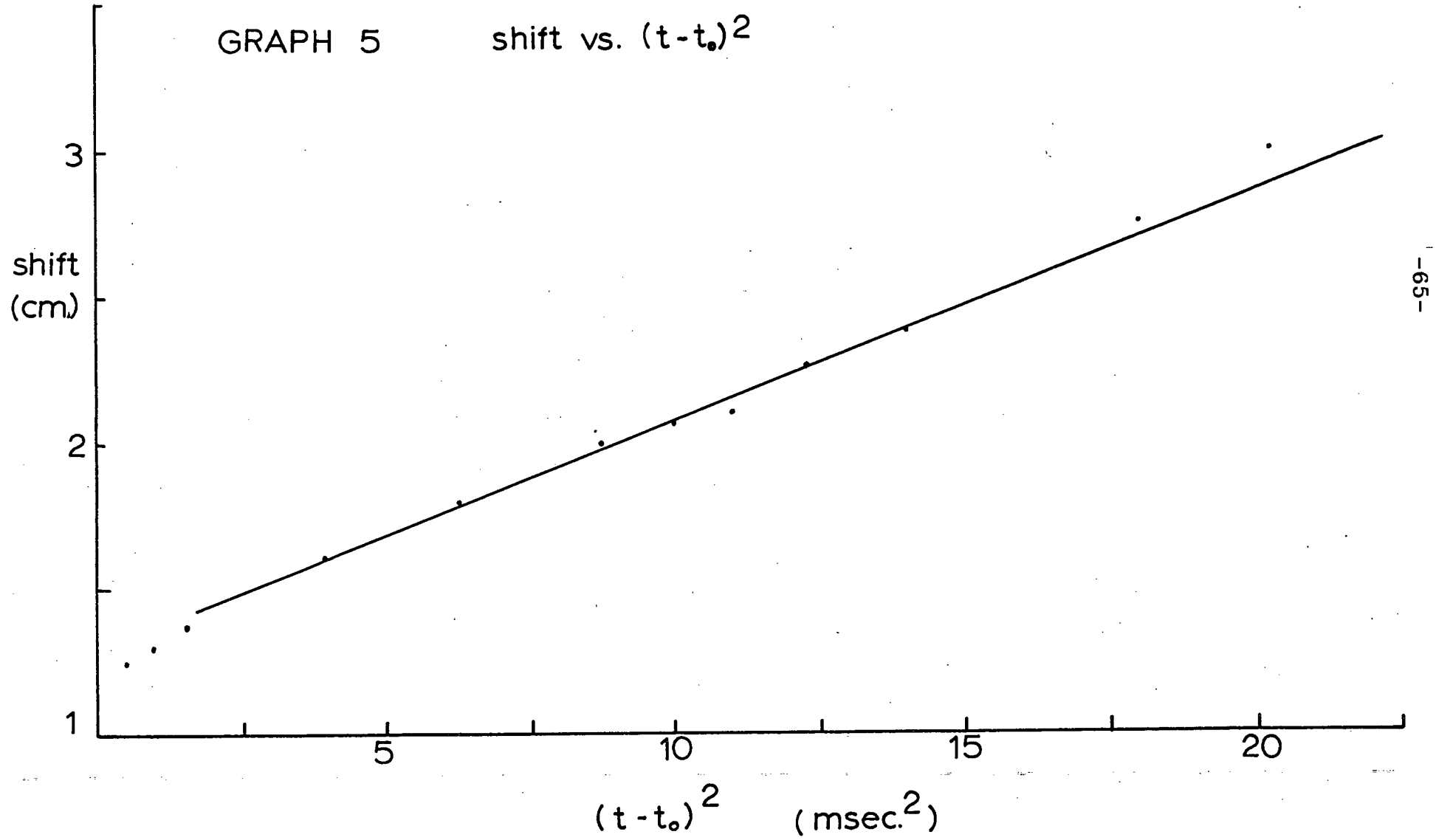
GRAPH 5
shift vs. $(t-t_o)^2$
shift (cm)
3
2
1
5
10
15
20
$(t-t_o)^2$ (msec.^{2})

The rest of the pictures were handled in a similar manner. The result of all the pictures is shown in Graph 6, where the growth rate ω is plotted as a function of the axial current. The error bars indicate the mean absolute deviation from the mean value taken from four to ten shots for each current.

The current was measured by measuring the voltage drop across the series limiting resistor. (see Fig. 4-12)

The theoretical fit shown in Graph 6 is taken from Graph 2. The value of k R for the jet is

$$kR_o = \frac{2\pi n}{L} R_i = 0.28$$ (cf. p. 58)

where n = 1, and L and R_i are as given before. The plot shows k R at 0.27, 0.28, and 0.29, giving the error limits on the theory due to uncertainties in the experimental parameters.

The results are in excellent agreement with the theory presented for the unstable jet in chapter 2 when one considers that for some currents, as few as four or five photographs were used to determine the average value and mean deviations of the growth rate.

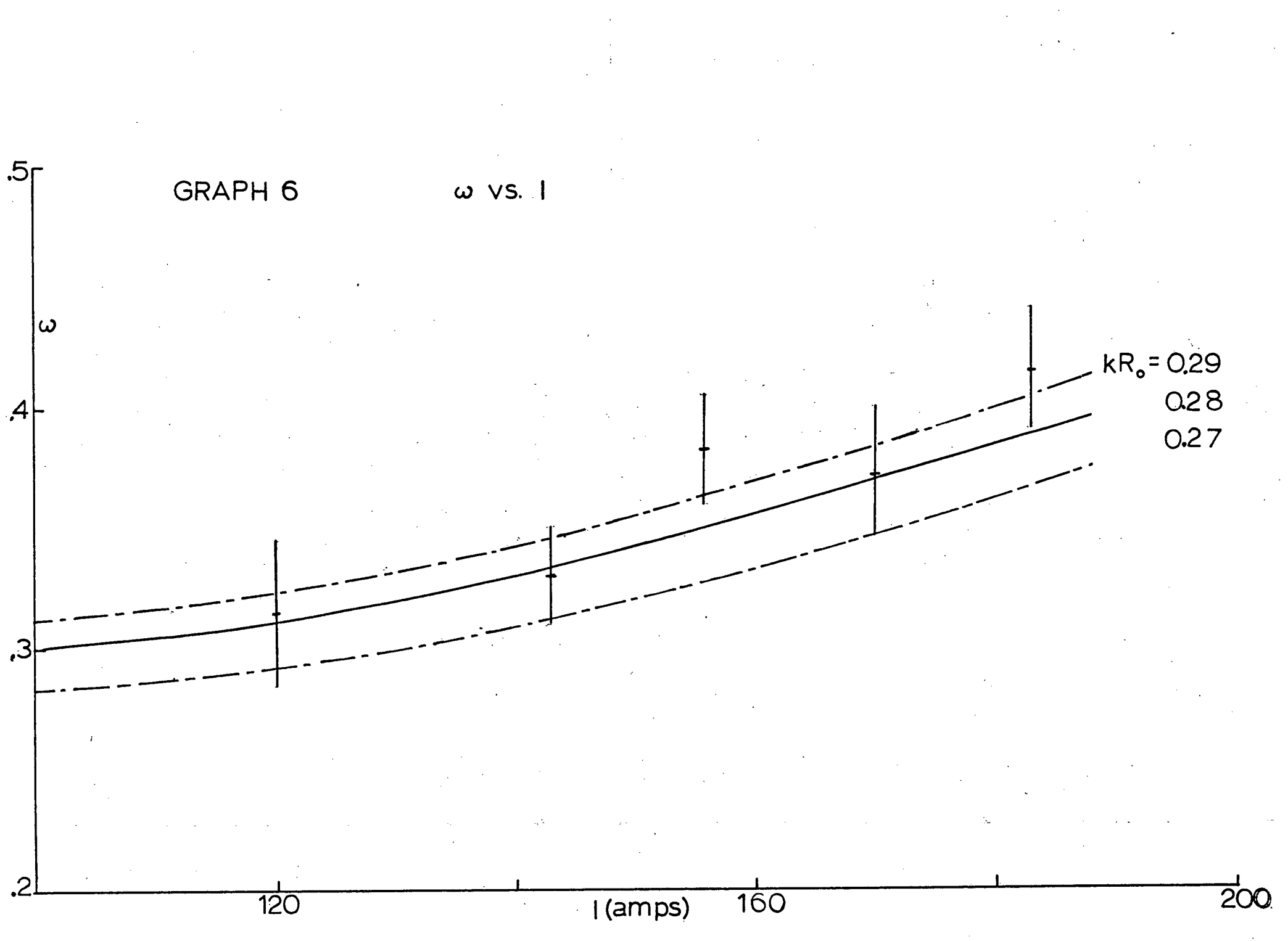
GRAPH 6
ω vs. I
.5
.4
.3
.2
ω
120
160
200
I (amps)
kR₀ = 0.29
0.28
0.27

Effects of Velocity

It is seen from Plate 3 that a definite stabilization is reached after a few milliseconds of growth of the pinch. Graph 7 shows how the total decrease in the radius at the pinch is related to the total axial current in the jet.

The velocity of the jet was measured by monitoring the flow rate out of the upper reservoir (having a constant mercury head above the nozzle.) If q is the flow rate out of the reservoir, and A is the area of the orfice, then the exit velocity of the jet is

$$v = \frac{q}{A}$$

For this system, the flow rate was 1.20 ml/sec. and the cross section of the nozzle is 0.058 cm^2 giving that the flow velocity is 30 cm/sec. This value includes the central rod in the jet.

Recall from chapter 3, that the decrease in radius at the pinch after stabilization is

$$\frac{a}{R_0} = \frac{\mu_0 I^2}{\rho R_0^2 V_0^2} \left(\frac{C\ell}{R_0}\right)^2 \quad ; \quad C\ell = 0.25\ mm$$

This is the theoretical curve shown in Graph 7. The error in the experimental points, and the error in the flow velocity, which is at least 10%, rule out any definite conclusions as to the effect of the central rod.

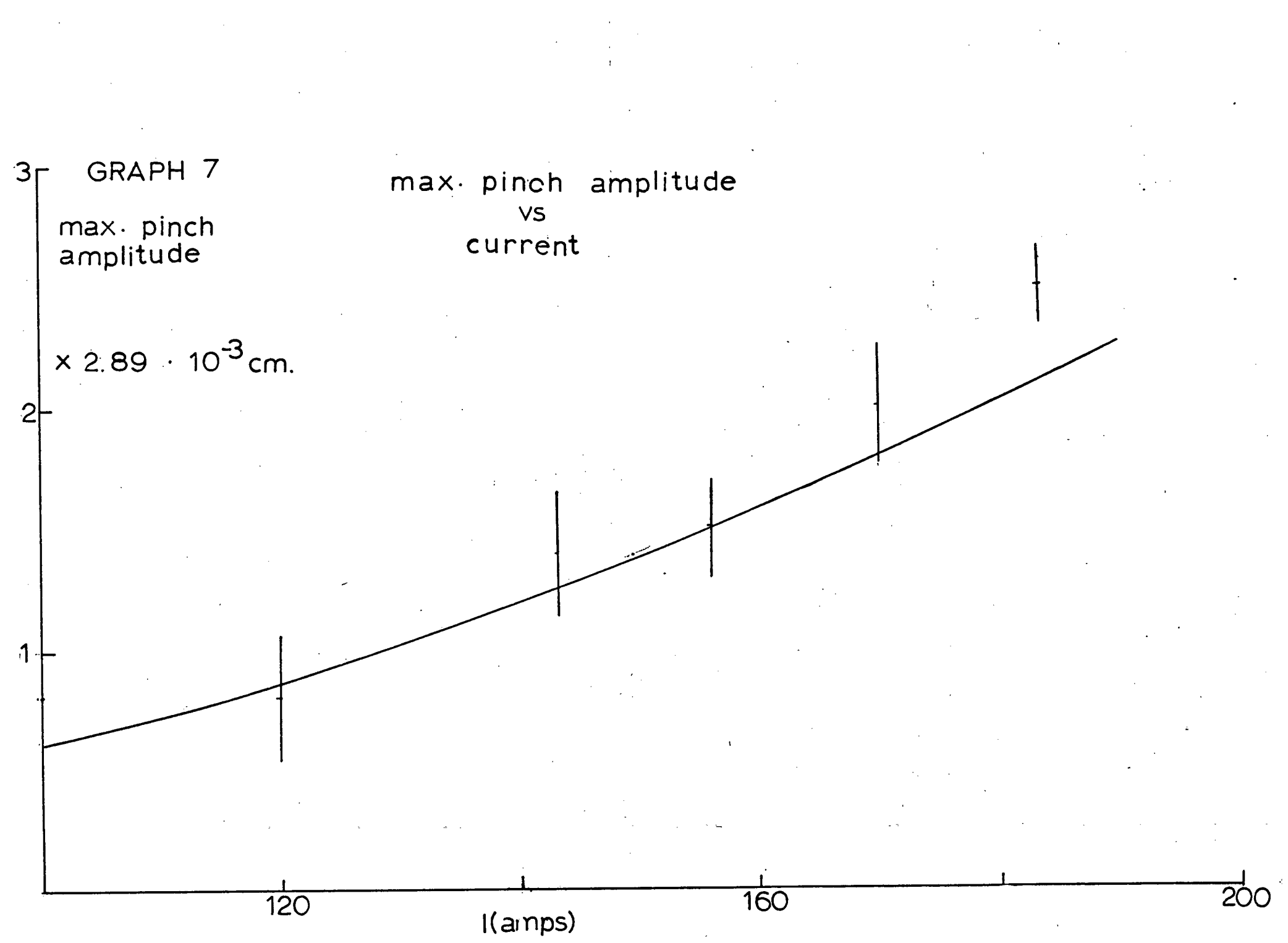
GRAPH 7
max. pinch amplitude
vs
current
max. pinch amplitude
x 2.89 · 10^-3 cm.
3
2
1
120
160
200
I(amps)

Concluding Summary

As can be seen by the preceeding discussion, the microwave resonant cavity technique is an excellent way of looking at surface instabilities on a cylindrical column of fluid. The maximum amplitude of wave seen is about a fiftieth of a millimeter. This is indeed a small amplitude in comparison with both the wavelength studied (about 3 cm.) and the column diameter. (about 2.5 mm.), so in fact, the most stringent linearization conditions that the theory require are easily satisfied.

The jet itself in the early stages of pinching is seen to have a surface configuration which is of the form

$$a \cosh \omega t \cos kz$$

and the initial growth rate has been verified to follow

$$\omega^2 = \frac{T(kR_o)(k^2R_o^2-1)I_1(kR_o)}{\rho R_o^3 \quad I_0(kR_o)} + \frac{\mu_0 I^2}{2\pi R_o^4 \rho}\left(\frac{I_2(kR_o)}{I_1(kR_o)} - \frac{I_1(kR_o)}{I_0(kR_o)}\right)$$

This is true at least in the current range 100 to 200 amps and for a kR product of about 0.3. Only future work will reveal the correctness of the above expression for the full range of parameters.

Now because the jet is moving with respect to the

source of the perturbation, an interesting effect is seen. The surface is seen to become stable again. That is, the pinch is seen to grow slower until eventually, further pinching action stops. A simple theory balancing magnetic pressure acting on the jet and the internal pressure resulting from the compression of the streamlines of the flow gives that the maximum pinch amplitude from the zero current equilibrium is

$$\frac{a}{R_o} = \frac{\mu_o I^2}{\rho R_o^2 V_o^2} \left(\frac{C\ell}{R_o}\right)^2 \quad ; \quad C\ell = 0.28\,\text{mm}.$$

The experiment indicates also that for an axial current in the range 100 to 200 amps this expression is quite correct. It should be pointed out that velocity dependence was not investigated, and complete verification of this simple theory needs this.

Chapter 6 What's Next?

Now that a technique for looking at surface waves on a fluid column has satisfactorily been tested, a whole new area of hydrodynamic instability research is opened up. Various E.H.D. and M.H.D. geometries immediately present themselves, a few of which I will now discuss.

(1) The immediate problem is to check the dispersion relation for all sausage modes of the axial current instability. This means that the full range of the product kR, where k is the instability wavenumber and R is the equilibrium radius of the column, must be looked into. This entails measuring the growth rate as a function of kR for several values of the axial current. This will probably be most conveniently achieved by using different cavity modes. (This varies the wavenumber looked at.)

The effect of the central perturbing wire should also be investigated. Several different wires should be tried for a given nozzle, and the corresponding growth rates compared.

The dependence of the second equilibrium on jet velocity should be further studied.

(2) The next step is to put an external axial magnetic field on the system. This could be done by mounting the cavity in the centre of a long solenoid. The magnetic field should have a stabilizing effect on the jet. (9)

A similar situation could be obtained by passing a different current down the perturbing wire than down the jet. This would mean that the jet would have to be insulated from the wire. However, the mercury has to wet the wire to get laminar flow, so a glass coated wire plated with copper may work. (see Fig. 6-1)

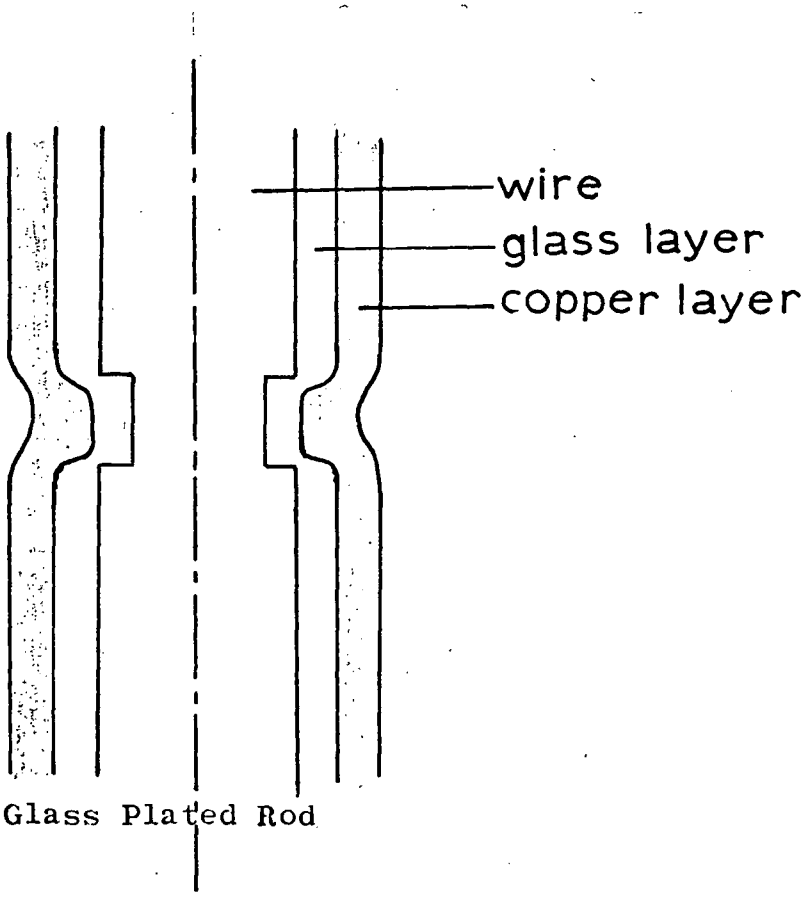

FIG. 6-1

Glass Plated Rod

(3) Another instability for investigation is the E.H.D. instability of the column. This means that the jet must be stressed by a strong radial electric field. Perhaps the best way of doing this is to use a cavity of small diameter, and charge up the whole cavity wall.

PLATES

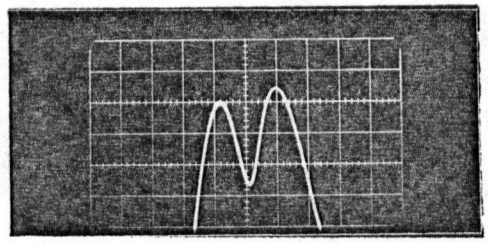

1. cavity resonance

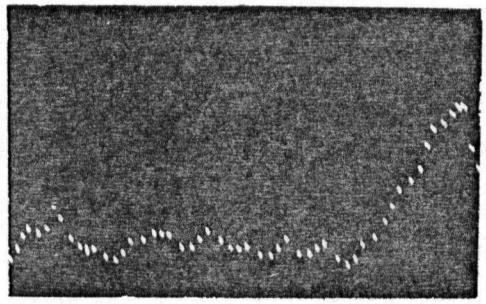

2. instability at 170 amps.

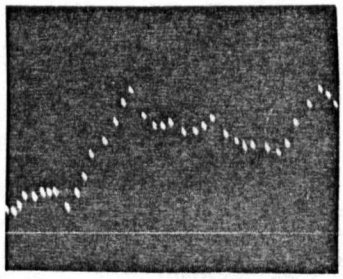

3. stability achieved at 170 amps.

References

(1) Carroll Lewis — Alice's Adventures in Wonderland, Charles E. Tuttle Co., 1968.

(2) Curzon F.L., Howard R. — Can. J Phy. 39, p1901, (1961)

(3) Curzon F.L., Ionides G.N. — Can. J Phy. 49, p458, (1971)

(4) Dättner A. — Arkiv for Fysik Bd 21, nr 7, (1961)

(5) Dattner A., Lehnert B., Lunquist S. — Second U.N. Conference on Peaceful Uses of Atomic Energy A/conf 15/D/1768 (19 May 1968)

(6) Howard R., Curzon F.L., Powell E.R. — J. Electronics and Control 14, no. 3, p 515, (1963)

(7) Lamb H. — Hydrodynamics, Dover Pub. Co. 1932

(8) Murty G.S. — Arkiv for Fysik Bd 18, nr 14, (1960)

(9) Murty G.S. — Arkiv for Fysik Bd 19, nr 35, (1961)

(10) Rayleigh — Scientific Papers ' Lord Rayleigh' 1, 58

(11) Rayleigh — Scientific Papers 'Lord Rayleigh' 1, 60

(12) Shercliff J.A. — A Textbook of Magnetohydrodynamics Permagon Press, 1961

(13) Slater J.C. — Microwave Electronics Dover Pub. Co., 1969

(14) Tandon J.N. Talwar S.P. — Plasma Physics 3, p261,(1961)

Appendix A-1 Hazards of Using Mercury

Mercury is a peculiar liquid in a great many ways. It is the only known metal that is liquid at 0 °C. The density of mercury is about 13.6 g/cm., double that of most metals. The surface tension of mercury is about 487 dynes/cm., significantly higher than most common liquids.

Another property of mercury is its toxicity. Mercury is lethal when it is present in the body in high concentrations, but simple precautions nearly eliminate this hazard. In this appendix, I shall attempt to describe some safety precautions that are mandatory in any experiment involving the use of mercury, and I shall also tell what to do if an accident occurs, and mercury is scattered to unwanted places.

(i) Containers for Mercury

In many experiments, mercury will have to be contained in some vessel either for transportation or storage. Special precautions must be observed for the construction of these vessels; these are summarized in what follows.

(1) Because of its high density, all containers for mercury must be sturdy, and all connections

such as hoses, must be securely fastened, and not just stuck together.

(2) It is well known that mercury forms amalgams with many common metals- brass, for instance. Thus if a brass container is to be used, it should be plated with nickel (or chromium) to a thickness of 0.003 inches or more.

(3) Because of the vapor hazard of mercury, all containers should be sealable and opened only for filling or draining, etc.

(4) Glass of course, is a good material for the construction of mercury containing vessels. However, one must be sure that the vessel can withstand the stresses placed on it by the weight of the mercury. If mercury is to be flowing at times, such as in a Mc leod gauge, one must make sure that a mercury hammer does not form and break the vessel.

(ii) General Laboratory Precautions

The first rule to remember when working with

mercury, is that it is poisonous, and its vapors can kill or seriously injure if taken into the body in sufficient quantities. The safety measures enforced on a personal level are strongly dependent on personal housekeeping practices. It must be remembered that once a mercury spill has occurred, it can never be totally cleaned up. The mercury tends to form tiny, often invisible droplets that sink into the cracks in the floor, scratches on the work bench, and generally into the most inaccessible places. This gives rise to the following suggestions.

(1) All experiments involving mercury should be conducted in rooms equipped with adequate enough ventilation to keep the vapor content in the air to less than the toxicity level of 0.1 mg/ m^3.

(2) The experiment should be designed in such a manner that if a spill occurs, the entire laboratory will not be contaminated with mercury droplets. This may mean building a floor level structure surrounding the apparatus, and sealing it floor-wise from the rest of the lab.

A convenient arrangement is to cover the floor under the apparatus with a sheet of polyvinyl chloride which is elevated a few inches at its edges. Any spill which may then occur, is confined to this giant tray under the apparatus. The sheet of plastic should be replaced periodically.

(3) Another necessary requirement is the routine monitoring of mercury vapor, especially frequent immediately after a spill. A 'mercury sniffer' Model K-23 manufactured by Beckmann Instruments Inc. was found satisfactory. I should point out that this seems to be about the most sensitive meter available, yet the toxic limit is only 10% of full scale. I think the final say should be left to the individual experimenter, as such a meter, in my opinion, cannot be used as the final authority.

What Do You Do With a Mercury Spill?

The obvious answer to this question is that you clean it up. However, the solution is not to sweep up the spilled mercury and throw it in a trash can.

This only removes the problem from sight. It is the purpose of this section to outline proper methods of clean up.

In case of an accidental spill of mercury (such as a broken manometer, a ruptured vessel, etc.) the following should be done immediately.

(1) Increase the ventilation in the room to maximum.

(2) Pick up all visible droplets and deposit then in a sealable container for later disposal. This can be satisfactorily done with a paper towel and a piece of brass shim stock. Some researchers recommend the use of a hypodermic syringe to suck up the mercury droplets. Do not use a vacuum cleaner since this would just vent the mercury throughout the lab.

(3) What to do next is open to some debate. The procedure used in this laboratory is to wash the floor (bench) with a solution of Hg-X. This is a sulfur containing compound manufactured by Acton Associates of Pennsylvania. This ccats the surface of any droplets with a sulfide that lowers the vapor pressure below the accepted threshold of danger.

The alternative, and better solution, is to have a removable floor surface.

(4) After cleanup is sufficient to put the vapor level below 0.1 mg/ cm^3, one can quit worrying. Frequent checks of the vapor pressure should be made to ensure that normal ventilation is adequate to keep the level to this.

After you are convinced that no danger exists, the cause of the spill must be corrected so that it will not happen again.

To date, there is no definite policy regarding the disposal of materials suspected as mercury carriers on this campus. These include the paper towels used to clean up the spills.

What has been done with these is that they have been sealed in doubled layered plastic bags and taken to the disposal grounds. This may not be the best way of disposal, but until some definite policy is reached, it stands at this.

References

Bidstrup P.L. Toxicity of Mercury and its Compounds
Elsevier Publishing Co., Holland, 1964.

Steere N.V. Handbook of Laboratory Safety
Chemical Rubber Co., U.S.A., 1967.

Appendix A-2 A Small Scale Nickel Plating Apparatus

If one wants to use brass components in a mercury environment, one has to plate the components with a continuous layer of some material which will not amalgamate with the mercury. This usually means nickel since it is the easiest and least costly plating material of this kind. In this appendix, I shall describe an apparatus which successfully plates nickel onto surfaces up to several square inches in area, and a plated thickness of a few thousandths of an inch.

Basically, nickel plating is accomplished be electroplating nickel out of a solution containing nickel ions. (see Fig. A-2-1)

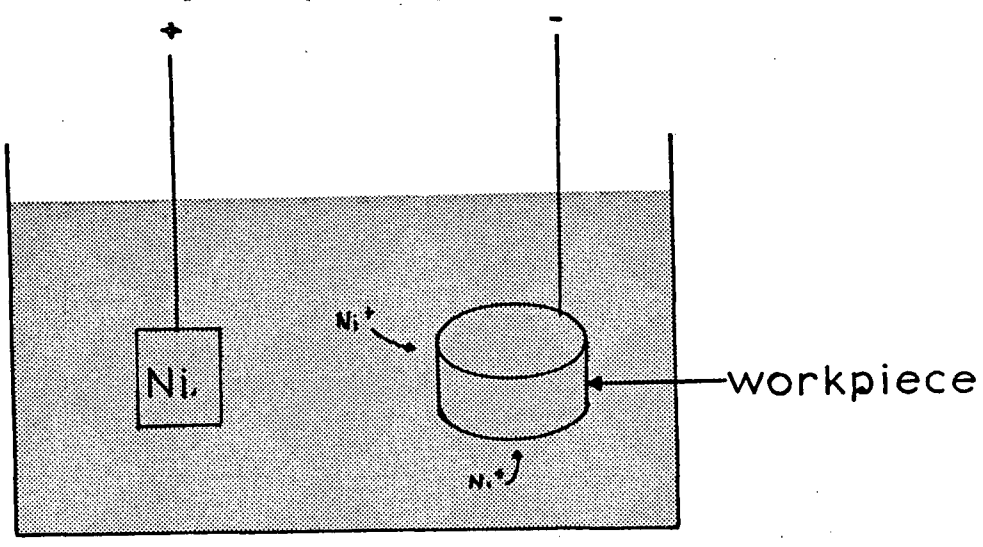

FIG. A-2-1 Nickel Plating Bath

The requirements for such a system are

(1) nickel ion bath

(2) nickel electrode

(3) d.c. power supply

The Nickel Bath

The nickel bath provides the nickel ions which are to be plated onto the workpiece. A typical bath known as the Watt's bath plates an even, bright, and hard nickel layer. Its constituents are

$Ni\ SO_4 \cdot 7\ H_2O$	300 g/l
$Ni\ Cl_2 \cdot 6\ H_2O$	60 g/l
Boric Acid	38 g/l

The nickel sulfate provides most of the plating ions. It is about the least expensive of the nickel salts that are not corrosive.

Nickel chloride is used to provide chloride ions to the solution. These ions permit a freer dissolving of the nickel electrode into solution. The electrode replaces the nickel ions that are plated out of solution.

The boric acid functions as a buffer. It tends to produce a smooth, hard finish. Without boric acid, the plated surface is often pitted, cracked, and highly stressed.

Nickel Electrode

The nickel electrode provides a means of returning the nickel ions to solution that are plated out. The electrode should be as pure as is economically possible.

Often these electrodes contain impurities which flake off during plating. It is customary to wrap the electrode in a 'cheese cloth' layer to prevent these flakes from entering the solution.

Often it will be found that the electrode shape required is difficult to shape out of pure nickel. I found that a heavy nickel plate on a brass electrode worked nicely.

Power Supply

A power supply capable of delivering up to 20 amps d.c. for up to ten hours continuously is necessary. The power supply I used was a Sorensen DCR 80-18.

To begin the nickel plating of the work piece, it is necessary to have a clean nonconducting container to hold the nickel ion solution. I found that a sink molded out of fibreglass worked well. The plating bath should be filtered into the clean container and then covered until it is used.

The electrode and work piece should be extremely clean before immersion into the bath. Sand blasting followed by electolysis in a solution of Na OH did the trick. The current for plating should be turned on and left on until the plating job is finished. I found that 5 to 10 amps was sufficient for work pieces of area less than a square foot.

If too much current is used, the plating will blister. Too little current result in impurities being plated out of solution first, giving a coat to the workpiece to which nickel may not stick. An even coating of'bubbles' leaving the work piece indicates the right current.

Reference

Gray A.G. Modern Electroplating
John Wiley and Sons, 1953.